UNIVERSIDAD DE CONCEPCIÓN

Centro de Investigación en Ingeniería Matemática (CI^{2}MA)

A virtual element method for Reissner-Mindlin plates

Lourenco Beirao-Da-Veiga, David Mora,
Gonzalo Rivera

PREPRINT 2016-14

SERIE DE PRE-PUBLICACIONES

A VIRTUAL ELEMENT METHOD FOR REISSNER-MINDLIN PLATES

L. BEIRÃO DA VEIGA*, D. MORA†, AND G. RIVERA‡

Abstract. We present a virtual element method for the Reissner–Mindlin plate bending problem which uses shear strain and deflection as discrete variables without the need of any reduction operator. The proposed method is conforming in $[H^1(\Omega)]^2 \times H^2(\Omega)$ and has the advantages of using general polygonal meshes and yielding a direct approximation of the shear strains. The rotations are then obtained as a simple postprocess from the shear strain and deflection. We prove convergence estimates with involved constants that are uniform in the thickness t of the plate. Finally, we report numerical experiments which allow us to assess the performance of the method.

Key words. Virtual element method, Reissner-Mindlin plates, error analysis, polygonal meshes.

AMS subject classifications. 65N30, 65N12, 74K20, 74S05, 65N15.

1. Introduction. The *Virtual Element Method* (VEM), introduced in [7, 8], is a recent generalization of the Finite Element Method which is characterized by the capability of dealing with very general polygonal/polyhedral meshes. The interest in numerical methods that can make use of general polytopal meshes has recently undergone a significant growth in the mathematical and engineering literature; among the large number of papers on this subject, we cite as a minimal sample [4, 7, 10, 23, 27, 38, 41, 42].

Indeed, polytopal meshes can be very useful for a wide range of reasons, including meshing of the domain (such as cracks) and data (such as inclusions) features, automatic use of hanging nodes, use of moving meshes, adaptivity. Moreover, the VEM presents the advantage to easily implement highly regular discrete spaces. Indeed, by avoiding the explicit construction of the local basis functions, the VEM can easily handle general polygons/polyhedrons without complex integrations on the element (see [8] for details on the coding aspects of the method). The Virtual Element Method has been applied successfully in a large range of problems, see for instance [1, 2, 6, 7, 8, 11, 13, 14, 15, 18, 21, 22, 30, 35, 36, 37, 43].

The Reissner–Mindlin theory is the most used model to approximate the deformation of a thin or moderately thick elastic plate. Nowadays, it is very well understood that the discretization of this problem poses difficulties due to the so called locking phenomenon when the thickness t is small with respect to the other dimensions of the plate. Nevertheless, adopting for instance a reduced integration or a mixed interpolation technique, this phenomenon can be avoided. Indeed, several families of methods have been rigorously shown to be free from locking and optimally convergent. We mention [29, 33] for a thorough description and further references.

Recently, a new approach to solve the Reissner–Mindlin bending problem has been presented in [9] by Beirão da Veiga et al. (see also [28, 32]). In this case a variational formulation of the plate bending problem is written terms of shear strain and deflection with the advantage that the "shear locking phenomenon" is avoided. A discretization of the problem by Isogeometric Analysis is proposed. Under some regularity assumptions on the exact solution, optimal error estimates with constants independent of the plate thickness are proved.

The aim of this paper is on developing a Virtual Element Method which applies to general polygonal (even non-convex) meshes for Reissner-Mindlin plates. We consider a variational formulation

* Dipartimento di Matematica e Applicazioni, Università di Milano-Bicocca, 20125 Milano, Italy. (lourenco.beirao@unimib.it).

† Departamento de Matemática, Universidad del Bío-Bío, Casilla 5-C, Concepción, Chile and CI^{2}MA, Universidad de Concepción, Concepción, Chile. (dmora@ubiobio.cl). Partially supported by CONICYT-Chile through FONDECYT project 1140791, by DIUBB through project 151408 GI/VC, and Anillo ANANUM, ACT1118, CONICYT (Chile).

‡ Centro de Investigación en Ingeniería Matemática (CI^{2}MA), Universidad de Concepción, Concepción, Chile and Departamento de Ingeniería Matemática, Universidad de Concepción, Concepción, Chile. (grivera@ing-mat.udec.cl). Partially supported by CONICYT (Chile) fellowship.

written in terms of shear strain and deflection presented in [9]. Here, we exploit the capability of VEM to built highly regular discrete spaces and propose a conforming $[H^1(\Omega)]^2 \times H^2(\Omega)$ discrete formulation, respectively for the shear strain and deflections. The resulting bilinear form is continuous and elliptic with appropriate t-dependent norms. This method makes use of a very simple set of degrees of freedom, namely 5 degrees of freedom per vertex of the mesh plus the number of edges, and approximates directly the transverse shear strain, which is distinctive of this approach. Moreover, the rotations are obtained as a simple postprocess from the shear strain and deflection. Under some regularity assumptions on the exact solution, optimal error estimates (in the natural norms of the adopted formulation) with constants independent of the plate thickness are proved for all the involved variables. In addition, we present error estimates in weaker norms using a duality argument. Finally, we point out that, differently from the finite element method where building globally $C^1(\Omega)$ functions is complicated, here the virtual deflection space can be built with a rather simple construction due to the flexibility of the virtual approach. In a summary, the advantages of the proposed method are the possibility to use general polygonal meshes and a better conformity with the limit Kirchhoff problem, ensuing from the $H^2(\Omega)$ approximation used for the discrete deflection.

The outline of this article is as follows: we introduce in Section 2 the Reissner-Mindlin plate model, first in terms of deflection and rotations variables and then in an equivalent form in terms of deflection and transverse shear strain variable. In Section 3, we present the discrete spaces for the shear strain and deflection, together with their properties, next, we construct the discrete bilinear forms and the loading term. We end this section with the presentation of the virtual element discrete formulation. In Section 4, we present the error analysis of the virtual scheme. In Section 5, we report a couple of numerical tests that allow us to assess the convergence properties of the method.

Throughout the paper, Ω is a generic Lipschitz bounded domain of $\mathbb{R}^2$. For $s \geq 0$, $\|\cdot\|_{s,\Omega}$ stands indistinctly for the norm of the Hilbertian Sobolev spaces $H^s(\Omega)$ or $[H^s(\Omega)]^2$ with the convention $H^0(\Omega) := L^2(\Omega)$. Finally, we employ $\mathbf{0}$ to denote a generic null vector and we will denote with C a generic constant which may take different values in different occurrences, and which is independent of the mesh parameter h and the plate thickness t.

2. Continuous problem. Consider an elastic plate of thickness t, $0 < t \leq 1$, with reference configuration $\Omega \times (-t/2, t/2)$, where Ω is a convex polygonal domain of $\mathbb{R}^2$ occupied by the mid-section of the plate. The deformation of the plate is described by means of the Reissner-Mindlin model in terms of the rotations $\boldsymbol{\theta} = (\theta_1, \theta_2)$ of the fibers initially normal to the plate mid-surface and the deflection w. We subdivide the boundary Γ of Ω in three disjoint parts such that,

$$\Gamma = \Gamma_c \cup \Gamma_s \cup \Gamma_f.$$

The plate is assumed to be clamped on Γ_c, simply supported on Γ_s and free on Γ_f. We assume that Γ_c has positive measure. We denote by $\boldsymbol{n}$ the outward unit normal vector to Γ, the following equations describe the plate response to a conveniently scaled transverse load g:

$$\left\{\begin{array}{lll} -\mathbf{div}\boldsymbol{\mathcal{C}}\varepsilon(\boldsymbol{\theta}) - \lambda t^{-2}(\nabla w - \boldsymbol{\theta}) = \mathbf{0} & & in\ \ \Omega, \\ -\operatorname{div}(\lambda t^{-2}(\nabla w - \boldsymbol{\theta})) = g & & in\ \ \Omega, \\ \boldsymbol{\theta} = \mathbf{0}, \quad w = 0 & & on\ \ \Gamma_c, \\ \boldsymbol{\mathcal{C}}\varepsilon(\boldsymbol{\theta})\boldsymbol{n} = \mathbf{0}, \quad w = 0 & & on\ \ \Gamma_s, \\ \boldsymbol{\mathcal{C}}\varepsilon(\boldsymbol{\theta})\boldsymbol{n} = \mathbf{0}, \quad (\boldsymbol{\theta} - \nabla w) = \mathbf{0} & & on\ \ \Gamma_f, \end{array}\right. \tag{2.1}$$

where $\lambda := Ek/2(1+\nu)$ is the shear modulus, with E being the Young modulus, ν the Poisson ratio, and k a correction factor, $\varepsilon(\boldsymbol{\theta}) := \frac{1}{2}(\nabla\boldsymbol{\theta} + (\nabla\boldsymbol{\theta})^t)$ is the standard strain tensor, and $\boldsymbol{\mathcal{C}}$ is the tensor of bending moduli, given by (for isotropic materials)

$$\boldsymbol{\mathcal{C}}\boldsymbol{\sigma} := \frac{E}{12(1-\nu^2)}\left((1-\nu)\boldsymbol{\sigma} + \nu\operatorname{tr}(\boldsymbol{\sigma})\mathbf{I}\right), \qquad \boldsymbol{\sigma} \in [L^2(\Omega)]^{2\times 2},$$

where $\operatorname{tr}(\boldsymbol{\sigma})$ is trace of $\boldsymbol{\sigma}$ and $\mathbf{I}$ is the identity tensor.

Let us consider the space

$$\widetilde{\boldsymbol{X}} := \{(v,\boldsymbol{\eta}) \in H^1(\Omega)\times[H^1(\Omega)]^2 : v = 0 \text{ on } \Gamma_c\cup\Gamma_s, \boldsymbol{\eta} = \boldsymbol{0} \text{ on } \Gamma_c\}.$$

By testing the system (2.1) with $(v,\boldsymbol{\eta}) \in \widetilde{\boldsymbol{X}}$, integrating by parts and using the boundary conditions, we write the following variational formulation:

PROBLEM 2.1. *Given $g \in L^2(\Omega)$, find $(w,\boldsymbol{\theta}) \in \widetilde{\boldsymbol{X}}$ such that*

$$a(\boldsymbol{\theta},\boldsymbol{\eta}) + b(\boldsymbol{\theta}-\nabla w, \boldsymbol{\eta}-\nabla v) = (g,v)_{0,\Omega} \qquad \forall (v,\boldsymbol{\eta}) \in \widetilde{\boldsymbol{X}},$$

where $(\cdot,\cdot)_{0,\Omega}$ denotes the inner-product in $L^2(\Omega)$, and the bilinear forms are given by

$$a(\boldsymbol{\theta},\boldsymbol{\eta}) := (\boldsymbol{\mathcal{C}}\varepsilon(\boldsymbol{\theta}),\varepsilon(\boldsymbol{\eta}))_{0,\Omega},$$
$$b(\boldsymbol{\theta},\boldsymbol{\eta}) := \lambda t^{-2}(\boldsymbol{\theta},\boldsymbol{\eta})_{0,\Omega}.$$

The following result states that the bilinear form appearing in Problem 2.1 is coercive (see [9, Proposition A.1]).

LEMMA 2.1. *There exists a positive constant α depending only on the material constants and the domain Ω such that:*

$$a(\boldsymbol{\eta},\boldsymbol{\eta}) + b(\boldsymbol{\eta}-\nabla v, \boldsymbol{\eta}-\nabla v) \geq \alpha\left(\|\boldsymbol{\eta}\|^2_{1,\Omega} + t^{-2}\|\boldsymbol{\eta}-\nabla v\|^2_{0,\Omega} + \|v\|^2_{1,\Omega}\right) \quad \forall (v,\boldsymbol{\eta}) \in \widetilde{\boldsymbol{X}}. \tag{2.2}$$

It is well known that the discretization of the Reissner-Mindlin equations have difficulties due to the so called locking phenomenon when the thickness t is small with respect to the other dimensions of the plate. To avoid this phenomenon we will introduce and analyze an alternative formulation of the problem that does not suffer from such a drawback. In order to simplify the notation, and without any loss of generality, we will assume $\lambda = 1$ in the following.

2.1. An equivalent variational formulation. The variational formulation that will be considered here, was introduced in the context of shells in [28, 32] and has been studied in [9] for Reissner-Mindlin plates using Isogeometric Analysis.

Now, we note that the equivalent formulation is derived by simply considering the following charge of variables:

$$(w,\boldsymbol{\theta}) \longleftrightarrow (w,\boldsymbol{\gamma}) \quad \text{with} \quad \boldsymbol{\theta} = \nabla w + \boldsymbol{\gamma}. \tag{2.3}$$

We note that the physical interpretation of the variable $\boldsymbol{\gamma}$ corresponds to the transverse shear strain.

The equivalent formulation will be obtained by using the change the variables (2.3) in Problem 2.1.

For the analysis we will consider the following t-dependent energy norm:

$$|||v,\boldsymbol{\tau}|||^2 := \|\boldsymbol{\tau}+\nabla v\|^2_{1,\Omega} + t^{-2}\|\boldsymbol{\tau}\|^2_{0,\Omega} + \|v\|^2_{1,\Omega}, \tag{2.4}$$

for all sufficiently regular functions $\boldsymbol{\tau} : \Omega \longrightarrow \mathbb{R}^2$ and $v : \Omega \longrightarrow \mathbb{R}$.

Now, we define the following variational spaces:

$$\widehat{\boldsymbol{X}} := \overline{C^\infty(\Omega)\times[C^\infty(\Omega)]^2}^{|||\cdot,\cdot|||};$$

$$\boldsymbol{X} := \{(v,\boldsymbol{\tau}) \in \widehat{\boldsymbol{X}} : v = 0 \text{ on } \Gamma_c\cup\Gamma_s, \nabla v + \boldsymbol{\tau} = \boldsymbol{0} \text{ on } \Gamma_c\}.$$

It is immediately verified that

$$H^2(\Omega)\times[H^1(\Omega)]^2 \subset \widehat{\boldsymbol{X}} \subset H^1(\Omega)\times[L^2(\Omega)]^2.$$

Moreover, note that the space $\boldsymbol{X}$ exactly corresponds to $\widetilde{\boldsymbol{X}}$ up to the change of variables (2.3).

Let us introduce the equivalent variational formulation for the Reissner-Mindlin model as follows:

PROBLEM 2.2. *Given $g \in L^2(\Omega)$, find $(w, \boldsymbol{\gamma}) \in \boldsymbol{X}$ such that*

$$a(\nabla w + \boldsymbol{\gamma}, \nabla v + \boldsymbol{\tau}) + b(\boldsymbol{\gamma}, \boldsymbol{\tau}) = (g, v)_{0,\Omega} \qquad \forall (v, \boldsymbol{\tau}) \in \boldsymbol{X}.$$

We have that Problem 2.2 is equivalent to Problem 2.1 up to the change of variables (2.3). As a consequence, we have the following coercivity property for the bilinear form on the left hand side of Problem 2.2 (see (2.2)):

$$a(\nabla v + \boldsymbol{\tau}, \nabla v + \boldsymbol{\tau}) + b(\boldsymbol{\tau}, \boldsymbol{\tau}) \geq \alpha |||v, \boldsymbol{\tau}|||^2 \quad \forall (v, \boldsymbol{\tau}) \in \boldsymbol{X}, \tag{2.5}$$

with same constant α. Moreover, bilinear forms $a(\cdot, \cdot)$ and $b(\cdot, \cdot)$ are bounded uniformly in t.

Therefore, Problem 2.2 has a unique solution $(w, \boldsymbol{\gamma}) \in \boldsymbol{X}$ and

$$|||w, \boldsymbol{\gamma}||| \leq C \|g\|_{0,\Omega}.$$

3. Virtual element discretization. We begin this section, by recalling the mesh construction and the assumptions considered to introduce the discrete virtual element spaces for the shear strain and deflection, together with their properties, next, we will introduce discrete bilinear forms and the loading term. Finally, we end this section with the presentation of the virtual element discretization of Problem 2.2.

3.1. Mesh regularity assumption. Let $\{\mathcal{T}_h\}_h$ be a sequence of decompositions of Ω into polygons E. Let h_E denote the diameter of the element E and $h := \max_{E \in \mathcal{T}_h} h_E$.

For the analysis, we will make the following assumptions as in [7, 12, 13]: there exists a positive real number $C_{\mathcal{T}}$ such that, for every h and every $E \in \mathcal{T}_h$,

$\mathbf{A}_1$: the ratio between the shortest edge and the diameter h_E of E is larger than $C_{\mathcal{T}}$;
$\mathbf{A}_2$: $E \in \mathcal{T}_h$ is star-shaped with respect to every point of a ball of radius $C_{\mathcal{T}} h_E$.

For any subset $S \subseteq \mathbb{R}^2$ and nonnegative integer k, we indicate by $\mathbb{P}_k(S)$ the space of polynomials of degree up to k defined on S. To keep the notation simpler, we denote by $\boldsymbol{n}$ a general normal unit vector; in each case, its precise definition will be clear from the context and we denote by $\boldsymbol{t}$ the tangent unit vector $\boldsymbol{t}$ defined as the anticlockwise rotation of $\boldsymbol{n}$.

To continue the construction of the discrete scheme, we need some preliminary definitions. First, we split the bilinear forms $a(\cdot, \cdot)$ and $b(\cdot, \cdot)$ introduced in the previous section as follows:

$$a\left(\nabla w + \boldsymbol{\gamma}, \nabla v + \boldsymbol{\tau}\right) = \sum_{E \in \mathcal{T}_h} a^E\left(\nabla w + \boldsymbol{\gamma}, \nabla v + \boldsymbol{\tau}\right) \quad \forall (w, \boldsymbol{\gamma}), (v, \boldsymbol{\tau}) \in \boldsymbol{X}, \tag{3.1}$$

$$b\left(\boldsymbol{\gamma}, \boldsymbol{\tau}\right) = \sum_{E \in \mathcal{T}_h} b^E(\boldsymbol{\gamma}, \boldsymbol{\tau}) \qquad \forall \boldsymbol{\gamma}, \boldsymbol{\tau} \in [H^1(\Omega)]^2, \tag{3.2}$$

with

$$a^E\left(\nabla w + \boldsymbol{\gamma}, \nabla v + \boldsymbol{\tau}\right) := \left(\boldsymbol{\mathcal{C}} \varepsilon(\nabla w + \boldsymbol{\tau}), \varepsilon(\nabla v + \boldsymbol{\gamma})\right)_{0,E}$$

and

$$b^E(\boldsymbol{\gamma}, \boldsymbol{\tau}) := t^{-2} (\boldsymbol{\gamma}, \boldsymbol{\tau})_{0,E}.$$

Finally, we define

$$\mathcal{A}((w, \boldsymbol{\gamma}), (v, \boldsymbol{\tau})) := a(\nabla w + \boldsymbol{\gamma}, \nabla v + \boldsymbol{\tau}) + b(\boldsymbol{\gamma}, \boldsymbol{\tau}) = \sum_{E \in \mathcal{T}_h} \mathcal{A}^E((w, \boldsymbol{\gamma}), (v, \boldsymbol{\tau})) \quad \forall (w, \boldsymbol{\gamma}), (v, \boldsymbol{\tau}) \in \boldsymbol{X},$$

where

$$\mathcal{A}^E((w,\boldsymbol{\gamma}),(v,\boldsymbol{\tau})) = a^E\left(\nabla w+\boldsymbol{\gamma},\nabla v+\boldsymbol{\tau}\right)) + b^E\left(\boldsymbol{\gamma},\boldsymbol{\tau}\right).$$

In order to construct the discrete scheme associated to Problem 2.2, in what follows, we will show that for each $h>0$ it is possible to build the following:

1. a discrete virtual space $\boldsymbol{X}_h \subseteq \boldsymbol{X}$ such that

$$\boldsymbol{X}_h := \{(v_h,\boldsymbol{\tau}_h) \in (W_h \times \mathbf{V}_h) : v_h = 0 \text{ on } \Gamma_c \cup \Gamma_s, \nabla v_h + \boldsymbol{\tau}_h = \mathbf{0} \text{ on } \Gamma_c\},$$

   in which the virtual spaces $W_h \subseteq H^2(\Omega)$ and $\mathbf{V}_h \subseteq [H^1(\Omega)]^2$;
2. a symmetric bilinear form $\mathcal{A}_h : \boldsymbol{X}_h \times \boldsymbol{X}_h \to \mathbb{R}$ which can be split as

$$\mathcal{A}_h((w_h,\boldsymbol{\gamma}_h),(v_h,\boldsymbol{\tau}_h)) := \sum_{E\in\mathcal{T}_h} \mathcal{A}_h^E((w_h,\boldsymbol{\gamma}_h),(v_h,\boldsymbol{\tau}_h)) \quad \forall (w_h,\boldsymbol{\gamma}_h),(v_h,\boldsymbol{\tau}_h) \in \boldsymbol{X}_h, \tag{3.3}$$

   with $\mathcal{A}_h^E(\cdot,\cdot)$ local bilinear forms on $\boldsymbol{X}_h|_E \times \boldsymbol{X}_h|_E$;
3. an element $g_h \in \boldsymbol{X}_h'$ and a discrete duality pair $\langle\cdot,\cdot\rangle_h$ in such a way that the following discrete problem: Find $(w_h,\boldsymbol{\gamma}_h) \in \boldsymbol{X}_h$ such that

$$\mathcal{A}_h((w_h,\boldsymbol{\gamma}_h),(v_h,\boldsymbol{\tau}_h)) = \langle g_h, v_h\rangle_h \qquad \forall (v_h,\boldsymbol{\tau}_h) \in \boldsymbol{X}_h, \tag{3.4}$$

   admits a unique solution $(w_h,\boldsymbol{\gamma}_h) \in \boldsymbol{X}_h$ and exhibits optimal approximation properties.

3.2. Discrete virtual spaces for shear strain and deflection. We introduce a pair of finite dimensional spaces for shear strain and deflection:

$$\mathbf{V}_h \subseteq [H^1(\Omega)]^2, \qquad W_h \subseteq H^2(\Omega).$$

First, we construct the shear strain virtual space $\mathbf{V}_h$, inspired from [2]. With this aim, we consider a simple polygon E and we define

$$\mathbb{B}_{\partial E} := \{\boldsymbol{\tau}_h \in [C^0(\partial E)]^2 : \boldsymbol{\tau}_h\cdot\boldsymbol{t}|_{\partial E} \in \mathbb{P}_2(e) \text{ and } \boldsymbol{\tau}_h\cdot\boldsymbol{n}|_{\partial E} \in \mathbb{P}_1(e) \ \ \forall e\in\partial E\}.$$

We then consider the finite dimensional space defined as follows:

$$\mathbf{V}_h^E := \{\boldsymbol{\tau}_h \in [H^1(E)]^2 : \operatorname{rot}\boldsymbol{\tau}_h \in \mathbb{P}_0(E), \boldsymbol{\tau}_h|_{\partial E} \in \mathbb{B}_{\partial E}, \boldsymbol{\tau}_h \text{ minimizes the } H^1\text{-seminorm}\}.$$

Note that the space $\mathbf{V}_h^E$ is well defined. Indeed, given a (piecewise polynomial) boundary value $\boldsymbol{\tau}_h|_{\partial E} \in [H^{1/2}(\partial E)]^2$, the associated function $\boldsymbol{\tau}_h$ inside the element E is obtained by solving the following well-posed problem:

$$\begin{cases} -\Delta\boldsymbol{\tau}_h + \mathbf{rot}\, s = \mathbf{0} \text{ in } E, \\ \operatorname{rot}\boldsymbol{\tau}_h = f \text{ with } f\in\mathbb{P}_0(E), \\ \boldsymbol{\tau}_h \text{ assigned in } \partial E, \end{cases} \tag{3.5}$$

where

$$f = \operatorname{rot}\boldsymbol{\tau}_h|_E = \frac{1}{|E|}\int_E \operatorname{rot}\boldsymbol{\tau}_h = \frac{1}{|E|}\int_{\partial E} \boldsymbol{\tau}_h\cdot\boldsymbol{t}.$$

It is important to observe that, since the functions in $\mathbf{V}_h^E$ are uniquely identified by their boundary values, $\dim(\mathbf{V}_h^E) = \dim(\mathbf{V}_h^E|_{\partial E})$, i.e., $\dim(\mathbf{V}_h^E) = 3N_E$, with N_E being the number of edges of E. This leads to introducing the following $3N_E$ degrees of freedom for the space $\mathbf{V}_h^E$:

- $\mathcal{V}_E^h$: the values of $\boldsymbol{\tau}_h$ (vector) at the vertices of E.

- $\mathcal{E}_E^h$: the value of the

$$\frac{1}{|e|}\int_e \boldsymbol{\tau}_h \cdot \boldsymbol{t} \quad \forall \text{ edge } e \in \partial E.$$

Moreover, we note that as a consequence of the definition $\mathbf{V}_h^E$, the output values of the two sets of degrees of freedom $\mathcal{V}_E^h$ and $\mathcal{E}_E^h$ are sufficient to uniquely determine $\boldsymbol{\tau}_h \cdot \boldsymbol{t}$ and $\boldsymbol{\tau}_h \cdot \boldsymbol{n}$ on the boundary of E, for any $\boldsymbol{\tau}_h \in \mathbf{V}_h^E$. Finally, we note that clearly $[\mathbb{P}_1(E)]^2 \subset \mathbf{V}_h^E$.

For every decomposition $\mathcal{T}_h$ of Ω into simple polygons E, we define the global space $\mathbf{V}_h$ without boundary conditions.

$$\mathbf{V}_h := \{\boldsymbol{\tau}_h \in [H^1(\Omega)]^2 : \boldsymbol{\tau}_h|_E \in \mathbf{V}_h^E \quad \forall E \in \mathcal{T}_h\}.$$

In agreement with the local choice of the degrees of freedom, in $\mathbf{V}_h$ we choose the following degrees of freedom:

- $\mathcal{V}^h$: the values of $\boldsymbol{\tau}_h$ (vector) at the vertices of $\mathcal{T}_h$.
- $\mathcal{E}^h$: the value of the

$$\frac{1}{|e|}\int_e \boldsymbol{\tau}_h \cdot \boldsymbol{t} \quad \forall \text{ edge } e \in \mathcal{T}_h.$$

Now, we will introduce the discrete virtual space W_h for the deflection, see also [21, 2]. With this aim, we first define the following finite dimensional space:

$$\begin{aligned} W_h^E := \{v_h \in H^2(E) : \Delta^2 v_h = 0, v_h|_{\partial E} \in C^0(\partial E), v_h|_{\partial E} \in \mathbb{P}_3(e), \\ \nabla v_h|_{\partial E} \in [C^0(\partial E)]^2 \text{ and } \partial_{\boldsymbol{n}} v_h|_{\partial E} \in \mathbb{P}_1(e) \quad \forall e \in \partial E\}, \end{aligned}$$

where Δ^2 represents the biharmonic operator. We observe that any $v_h \in W_h^E$ satisfy the following conditions:

- the trace on the boundary of E is continuous and on each edge is a polynomial of degree 3;
- the gradient on the boundary is continuous and on each edge its normal (respectively tangential) component is a polynomial of degree 1 (respectively 2);
- inside E satisfy the biharmonic equation $\Delta^2 v_h = 0$;
- $\mathbb{P}_2(E) \subseteq W_h^E$.

We choose in W_h^E the degrees of freedom introduced in [3, Section 2.2], namely:

- $\mathcal{W}_E^h$: The values of v_h and ∇v_h at the vertices of E.

We note that as a consequence of the definition W_h^E, the degrees of freedom $\mathcal{W}_E^h$ are sufficient to uniquely determine v_h and ∇v_h on the boundary of E.

We now present the global virtual space for the deflection: for every decomposition $\mathcal{T}_h$ of Ω into simple polygons E, we define (without boundary conditions).

$$W_h := \{v_h \in H^2(\Omega) : v_h|_E \in W_h^E \quad \forall E \in \mathcal{T}_h\}.$$

In agreement with the local choice of the degrees of freedom, in W_h we choose the following degrees of freedom:

- $\mathcal{W}^h$: the values of v_h and ∇v_h at the vertices of $\mathcal{T}_h$.

As a consequence of the definition of local virtual spaces $\mathbf{V}_h^E$ and W_h^E, we have the following result which will be used in the forthcoming analysis.

PROPOSITION 3.1. *Let E be a simple polygon with N_E edges. Then $\nabla W_h^E \subseteq \mathbf{V}_h^E$.*

Proof. Let $v_h \in W_h^E$, then we have that: $v_h \in H^2(E)$, $\Delta^2 v_h = 0$, $v_h|_e \in \mathbb{P}_3(e)$ and $\nabla v_h \cdot \boldsymbol{n}|_e \in \mathbb{P}_1(e)$ for all $e \in \partial E$. Hence, $\nabla v_h \in [H^1(E)]^2$, $\nabla v_h \cdot \boldsymbol{t}|_e \in \mathbb{P}_2(e)$ and $\nabla v_h \cdot \boldsymbol{n}|_e \in \mathbb{P}_1(e)$ for all $e \in \partial E$, i.e, $\nabla v_h|_{\partial E} \in \mathbb{B}_{\partial E}$. Moreover, $\mathrm{rot}(\nabla v_h) = 0 \in \mathbb{P}_0(E)$. On the other hand, we have that

$$0 = \Delta^2 v_h = \Delta\left(\Delta v_h\right) = \Delta\left(\mathrm{div}(\nabla v_h)\right) = \mathrm{div}\left(\Delta(\nabla v_h)\right).$$

Since a star-shaped polygon E is simply connected, there exists $q \in H^1(E)$ such that $\Delta(\nabla v_h) = \mathbf{rot}\, q$. Thus, ∇v_h satisfies (3.5) and therefore $\nabla v_h \in \mathbf{V}_h^E$. The proof is complete. □

Finally, once we have defined $\mathbf{V}_h$ and W_h, we are able to introduce our virtual element space $\boldsymbol{X}_h$.

$$\boldsymbol{X}_h := \{(v_h, \boldsymbol{\tau}_h) \in W_h \times \mathbf{V}_h\} \cap \boldsymbol{X}.$$

3.3. Bilinear forms and the loading term. In this section we will discuss the construction of the discrete version of the local bilinear forms $a^E(\cdot,\cdot)$ (cf (3.1)) and $b^E(\cdot,\cdot)$ (cf (3.2)), which will be used to built the local bilinear form appearing in (3.3). Moreover, we will discuss the construction of the loading term appearing in (3.4).

We define the projector $\Pi_\varepsilon^E : \mathbf{V}_h^E \longrightarrow [\mathbb{P}_1(E)]^2 \subset \mathbf{V}_h^E$ for each $\boldsymbol{\tau}_h \in \mathbf{V}_h^E$ as the solution of

$$\text{(3.6)} \qquad \begin{cases} a^E(\boldsymbol{p}, \Pi_\varepsilon^E \boldsymbol{\tau}_h) = a^E(\boldsymbol{p}, \boldsymbol{\tau}_h) \quad \forall \boldsymbol{p} \in [\mathbb{P}_1(E)]^2, \\ \big\langle\big\langle \boldsymbol{p}, \Pi_\varepsilon^E \boldsymbol{\tau}_h \big\rangle\big\rangle = \langle\langle \boldsymbol{p}, \boldsymbol{\tau}_h \rangle\rangle \quad \forall \boldsymbol{p} \in ker(a^E(\cdot,\cdot)), \end{cases}$$

where for all $\mathbf{r}_h, \mathbf{s}_h$ in $\mathbf{V}_h^E$

$$\langle\langle \mathbf{r}_h, \mathbf{s}_h \rangle\rangle := \frac{1}{N_E} \sum_{i=1}^{N_E} \mathbf{r}_h(\mathsf{v}_i) \cdot \mathbf{s}_h(\mathsf{v}_i), \quad \mathsf{v}_i = \text{ vertices of } E,\ 1 \le i \le N_E.$$

We note that the second equation in (3.6) is needed for the problem to be well-posed. In fact, it is easy to check that it returns one (and only one) function $\Pi_\varepsilon^E \boldsymbol{\tau}_h \in [\mathbb{P}_1(E)]^2$. Moreover, we observe that the local degrees of freedom allow us to compute exactly the right hand side of (3.6). Indeed, for all $\boldsymbol{p} \in [\mathbb{P}_1(E)]^2$, we have

$$\begin{aligned} a^E(\boldsymbol{p}, \boldsymbol{\tau}_h) = \int_E \boldsymbol{\mathcal{C}}\varepsilon(\boldsymbol{p}) \colon \varepsilon(\boldsymbol{\tau}_h) &= -\int_E \mathbf{div}(\boldsymbol{\mathcal{C}}\varepsilon(\boldsymbol{p})) \cdot \boldsymbol{\tau}_h + \int_{\partial E} (\boldsymbol{\mathcal{C}}\varepsilon(\boldsymbol{p})\boldsymbol{n}) \cdot \boldsymbol{\tau}_h \\ &= \int_{\partial E} (\boldsymbol{\mathcal{C}}\varepsilon(\boldsymbol{p})\boldsymbol{n}) \cdot \boldsymbol{\tau}_h, \end{aligned}$$

where we have used that $\mathbf{div}(\boldsymbol{\mathcal{C}}\varepsilon(\boldsymbol{p})) = \mathbf{0}$. Therefore, since the functions $\boldsymbol{\tau}_h \in \mathbf{V}_h^E$ are known explicitly on the boundary, the right hand side of (3.6) can be computed exactly without knowing $\boldsymbol{\tau}_h$ in the interior of E. As a consequence, the projection operator Π_ε^E is computable solely on the basis of the degrees of freedom values.

Let $\Pi_0^E : \mathbf{V}_h^E \to [\mathbb{P}_0(E)]^2$ be the $[L^2(E)]^2$-projector, defined by

$$\int_E \Pi_0^E \boldsymbol{\tau}_h \cdot \boldsymbol{p}_0 = \int_E \boldsymbol{\tau}_h \cdot \boldsymbol{p}_0 \quad \forall \boldsymbol{p}_0 \in [\mathbb{P}_0(E)]^2.$$

We note that as before, the right hand side above is computable. In fact, we consider a simple polygon E with barycenter $\mathbf{x}_E = (x_E, y_E)^t$ and we have that any $\boldsymbol{p}_0 \in [\mathbb{P}_0(E)]^2$ can be written as $\boldsymbol{p}_0 = \alpha(1,0)^t + \beta(0,1)^t = \alpha\,\mathbf{rot}(y - y_E) + \beta\,\mathbf{rot}(x_E - x)$. Thus, for all $\boldsymbol{\tau}_h \in \mathbf{V}_h^E$ we have

$$\begin{aligned} \int_E \boldsymbol{\tau}_h \cdot (1,0)^t = \int_E \boldsymbol{\tau}_h \cdot \mathbf{rot}(y - y_E) &= \int_E \operatorname{rot} \boldsymbol{\tau}_h (y - y_E) - \int_{\partial E} (\boldsymbol{\tau}_h \cdot \boldsymbol{t})\,(y - y_E) \\ &= \operatorname{rot} \boldsymbol{\tau}_h \int_E (y - y_E) - \int_{\partial E} (\boldsymbol{\tau}_h \cdot \boldsymbol{t})\,(y - y_E) = -\int_{\partial E} (\boldsymbol{\tau}_h \cdot \boldsymbol{t})\,(y - y_E), \end{aligned}$$

where we have used that for $\boldsymbol{\tau}_h \in \mathbf{V}_h^E$, $\operatorname{rot} \boldsymbol{\tau}_h \in \mathbb{P}_0(E)$. Using the same arguments, we get

$$\int_E \boldsymbol{\tau}_h \cdot (0,1)^t = -\int_{\partial E} (\boldsymbol{\tau}_h \cdot \boldsymbol{t})\,(x_E - x),$$

which shows that $\Pi_0^E \boldsymbol{\tau}_h$ is computable solely on the basis of the degree of freedom values.

Let now $S^E(\cdot,\cdot)$ and $S_0^E(\cdot,\cdot)$ be any symmetric positive definite bilinear forms to be chosen as to satisfy

$$c_0 a^E(\boldsymbol{\tau}_h,\boldsymbol{\tau}_h) \leq S^E(\boldsymbol{\tau}_h,\boldsymbol{\tau}_h) \leq c_1 a^E(\boldsymbol{\tau}_h,\boldsymbol{\tau}_h) \quad \forall \boldsymbol{\tau}_h \in \mathbf{V}_h^E \ \text{ with } \Pi_\varepsilon^E \boldsymbol{\tau}_h = 0, \tag{3.7}$$

$$\tilde{c}_0 b^E(\boldsymbol{\tau}_h,\boldsymbol{\tau}_h) \leq S_0^E(\boldsymbol{\tau}_h,\boldsymbol{\tau}_h) \leq \tilde{c}_1 b^E(\boldsymbol{\tau}_h,\boldsymbol{\tau}_h) \quad \forall \boldsymbol{\tau}_h \in \mathbf{V}_h^E, \tag{3.8}$$

for some positive constants c_0, c_1, $\tilde{c}_0$ and $\tilde{c}_1$ depending only on the constant $C_{\mathcal{T}}$ from mesh assumptions $\mathbf{A}_1$ and $\mathbf{A}_2$. Then, we introduce on each element E the local (and computable) bilinear forms

$$\begin{aligned} a_h^E(\boldsymbol{\gamma}_h,\boldsymbol{\tau}_h) &:= a^E(\Pi_\varepsilon^E\boldsymbol{\gamma}_h,\Pi_\varepsilon^E\boldsymbol{\tau}_h) + S^E(\boldsymbol{\gamma}_h - \Pi_\varepsilon^E\boldsymbol{\gamma}_h, \boldsymbol{\tau}_h - \Pi_\varepsilon^E\boldsymbol{\tau}_h) \qquad \boldsymbol{\gamma}_h,\boldsymbol{\tau}_h \in \mathbf{V}_h^E, \\ b_h^E(\boldsymbol{\gamma}_h,\boldsymbol{\tau}_h) &:= b^E(\Pi_0^E\boldsymbol{\gamma}_h,\Pi_0^E\boldsymbol{\tau}_h) + S_0^E(\boldsymbol{\gamma}_h - \Pi_0^E\boldsymbol{\gamma}_h, \boldsymbol{\tau}_h - \Pi_0^E\boldsymbol{\tau}_h) \qquad \boldsymbol{\gamma}_h,\boldsymbol{\tau}_h \in \mathbf{V}_h^E. \end{aligned}$$

Now, we define in a natural way

$$a_h(\boldsymbol{\gamma}_h,\boldsymbol{\tau}_h) := \sum_{E\in\mathcal{T}_h} a_h^E(\boldsymbol{\gamma}_h,\boldsymbol{\tau}_h), \qquad b_h(\boldsymbol{\gamma}_h,\boldsymbol{\tau}_h) := \sum_{E\in\mathcal{T}_h} b_h^E(\boldsymbol{\gamma}_h,\boldsymbol{\tau}_h) \qquad \boldsymbol{\gamma}_h,\boldsymbol{\tau}_h \in \mathbf{V}_h.$$

The construction of $a_h^E(\cdot,\cdot)$ and $b_h^E(\cdot,\cdot)$ guarantees the usual consistency and stability properties of VEM, as noted in the Proposition below. Since the proof is simple and follows standard arguments in the Virtual Element literature, it is omitted.

PROPOSITION 3.2. *The local bilinear forms $a_h^E(\cdot,\cdot)$ and $b_h^E(\cdot,\cdot)$ on each element E satisfy*

- *Consistency: for all $h>0$ and for all $E\in\mathcal{T}_h$ we have that*

$$a_h^E(\boldsymbol{p},\boldsymbol{\tau}_h) = a^E(\boldsymbol{p},\boldsymbol{\tau}_h) \quad \forall \boldsymbol{p}\in[\mathbb{P}_1(E)]^2,\ \forall \boldsymbol{\tau}_h\in\mathbf{V}_h^E; \tag{3.9}$$

$$b_h^E(\boldsymbol{p}_0,\boldsymbol{\tau}_h) = b^E(\boldsymbol{p}_0,\boldsymbol{\tau}_h) \quad \forall \boldsymbol{p}_0\in[\mathbb{P}_0(E)]^2,\ \forall \boldsymbol{\tau}_h\in\mathbf{V}_h^E. \tag{3.10}$$

- *Stability: there exist positive constants α_*, α^*, β_* and β^*, independent of h and E, such that*

$$\alpha_* a^E(\boldsymbol{\tau}_h,\boldsymbol{\tau}_h) \leq a_h^E(\boldsymbol{\tau}_h,\boldsymbol{\tau}_h) \leq \alpha^* a^E(\boldsymbol{\tau}_h,\boldsymbol{\tau}_h) \quad \forall \boldsymbol{\tau}_h\in\mathbf{V}_h^E, \quad \forall E\in\mathcal{T}_h, \tag{3.11}$$

$$\beta_* b^E(\boldsymbol{\tau}_h,\boldsymbol{\tau}_h) \leq b_h^E(\boldsymbol{\tau}_h,\boldsymbol{\tau}_h) \leq \beta^* b^E(\boldsymbol{\tau}_h,\boldsymbol{\tau}_h) \quad \forall \boldsymbol{\tau}_h\in\mathbf{V}_h^E, \quad \forall E\in\mathcal{T}_h. \tag{3.12}$$

We note that as a consequence of (3.11) and (3.12), the bilinear forms $a_h^E(\cdot,\cdot)$ and $b_h^E(\cdot,\cdot)$ are bounded with respect to the H^1 and L^2 norms, respectively.

We now discuss the construction of the loading term. For every $E\in\mathcal{T}_h$ we approximate the data g by a piecewise constant function g_h on each element E defined as the $L^2(E)$-projection of the load g (denoted by $\bar{g}_E$). Let the loading term

$$\langle g_h, v_h\rangle_h := \sum_{E\in\mathcal{T}_h} \bar{g}_E \sum_{i=1}^{N_E} v_h(\mathsf{v}_i)\omega_E^i. \tag{3.13}$$

where $\mathsf{v}_1,\ldots,\mathsf{v}_{N_E}$ are the vertices of E and $\omega_E^1,\ldots,\omega_E^{N_E}$ are positive weights chosen to provide the exact integral on E when applied to linear functions.

3.4. Discrete problem. The results of the previous sections allow us to introduce the discrete VEM in shear strain-deflection formulation for the approximation of the continuous Reissner-Mindlin formulation presented in Problem 2.2.

With this aim, we first note that since $\nabla W_h^E \subset \mathbf{V}_h^E$ (see Proposition 3.1), the operator Π_ε^E can be also applied to ∇v_h for all $v_h\in W_h^E$. Hence, we introduce the following VEM discretization for the approximation of Problem 2.2.

PROBLEM 3.1. *Find $(w_h,\boldsymbol{\gamma}_h)\in\boldsymbol{X}_h$ such that*

$$a_h(\nabla w_h+\boldsymbol{\gamma}_h, \nabla v_h+\boldsymbol{\tau}_h) + b_h(\boldsymbol{\gamma}_h,\boldsymbol{\tau}_h) = \langle g_h, v_h\rangle_h \qquad \forall (v_h,\boldsymbol{\tau}_h)\in\boldsymbol{X}_h. \tag{3.14}$$

The next lemma shows that the problem above is coercive in the $|||\cdot|||$ norm.

LEMMA 3.3. *There exists $\beta > 0$, independent of h and t such that*

$$a_h(\nabla v_h + \boldsymbol{\tau}_h, \nabla v_h + \boldsymbol{\tau}_h) + b_h(\boldsymbol{\tau}_h, \boldsymbol{\tau}_h) \geq \beta \, |||(v_h, \boldsymbol{\tau}_h)|||^2 \qquad \forall (v_h, \boldsymbol{\tau}_h) \in \boldsymbol{X}_h.$$

Proof. Thanks to (3.11), (3.12) and (2.5), we have that

$$a_h(\nabla v_h + \boldsymbol{\tau}_h, \nabla v_h + \boldsymbol{\tau}_h) + b_h(\boldsymbol{\tau}_h, \boldsymbol{\tau}_h) \geq C_* \left(a(\nabla v_h + \boldsymbol{\tau}_h, \nabla v_h + \boldsymbol{\tau}_h) + b(\boldsymbol{\tau}_h, \boldsymbol{\tau}_h)\right) \geq \beta \, |||(v_h, \boldsymbol{\tau}_h)|||^2,$$

with $\beta := \min\{C_*, \alpha\}$. □ We deduce immediately from Lemma 3.3 that Problem 3.1 is well-posed.

Remark 3.1. *The solution of Problem 2.2 delivers the shear strain and deflection. In addition, it is possible to readily obtain the rotations $\boldsymbol{\theta}$ by recalling* (2.3)*. At the discrete level, this strategy corresponds to computing the rotations as a post-processing of the shear strain and deflection. If $(w_h, \boldsymbol{\gamma}_h) \in \boldsymbol{X}_h$ is the unique solutions of Problem 3.1, then the function*

$$\boldsymbol{\theta}_h = \nabla w_h + \boldsymbol{\gamma}_h,$$

is an approximation of the rotations. The accuracy of such approximation will be established in the following section.

4. Convergence analysis. In the present section, we develop an error analysis for the discrete virtual element scheme presented in Section 3.4. For the forthcoming analysis, we will assume that the mesh assumptions $\mathbf{A}_1$ and $\mathbf{A}_2$, introduced in Section 3.1, are satisfied.

For the analysis we will introduce the broken H^1-norm:

$$\|v\|_{1,h,\Omega}^2 := \sum_{E \in \mathcal{T}_h} \|v\|_{1,E}^2,$$

which is well defined for every $v \in L^2(\Omega)$ such that $v|_E \in H^1(E)$ for all polygon $E \in \mathcal{T}_h$.

Moreover, we have the following propositions, which are derived by interpolation between Sobolev spaces (see for instance [31, Theorem I.1.5] from the analogous result for integer values of s. In its turn, the result for integer values is stated in [7, Proposition 4.2] and follows from the classical Scott-Dupont theory (see [17]).

PROPOSITION 4.1. *There exists a constant $C > 0$, such that for every $v \in H^s(E)$ there exists $v_\Pi \in \mathbb{P}_k(E)$, $k \geq 0$ such that*

$$|v - v_\Pi|_{l,E} \leq C h_E^{s-l} |v|_{s,E} \quad 0 \leq s \leq k+1, l = 0, \ldots, s.$$

PROPOSITION 4.2. *There exists a constant $C > 0$, such that for every $\boldsymbol{\tau} \in [H^s(E)]^2$ there exists $\boldsymbol{\tau}_\Pi \in [\mathbb{P}_k(E)]^2$, $k \geq 0$ such that*

$$|\boldsymbol{\tau} - \boldsymbol{\tau}_\Pi|_{l,E} \leq C h_E^{s-l} |\boldsymbol{\tau}|_{s,E} \quad 0 \leq s \leq k+1, l = 0, \ldots, s.$$

The first step is to establish the following result.

LEMMA 4.3. *Let $(w, \boldsymbol{\gamma}) \in \boldsymbol{X}$ be the unique solution to the continuous Problem 2.2 and let $\boldsymbol{\theta} := \nabla w + \boldsymbol{\gamma}$. Let $(w_h, \boldsymbol{\gamma}_h) \in \boldsymbol{X}_h$ be the unique solution to the discrete Problem 3.1. Then, for any $(w_I, \boldsymbol{\gamma}_I) \in \boldsymbol{X}_h$ and $(\boldsymbol{\theta}_\Pi, \boldsymbol{\gamma}_\Pi, \boldsymbol{\gamma}_0) \in [L^2(\Omega)]^6$ such that $\boldsymbol{\theta}_\Pi|_E \in [\mathbb{P}_1(E)]^2$, $\boldsymbol{\gamma}_\Pi|_E \in [\mathbb{P}_1(E)]^2$ and $\boldsymbol{\gamma}_0|_E \in [\mathbb{P}_0(E)]^2$ for all $E \in \mathcal{T}_h$, there exists $C > 0$ independent of h and t such that*

$$\begin{aligned} |||w - w_h, \boldsymbol{\gamma} - \boldsymbol{\gamma}_h||| \leq C \big(& t^{-1} \left(\|\boldsymbol{\gamma} - \boldsymbol{\gamma}_I\|_{0,\Omega} + \|\boldsymbol{\gamma}_0 - \boldsymbol{\gamma}\|_{0,\Omega} \right) + \|\boldsymbol{\gamma} - \boldsymbol{\gamma}_I\|_{1,\Omega} + h\|g\|_{0,\Omega} \\ & + \|\boldsymbol{\theta} - \boldsymbol{\theta}_\Pi\|_{1,h,\Omega} + \|\nabla w - \nabla w_I\|_{1,\Omega} \big). \end{aligned}$$

Proof. We set $\boldsymbol{\delta_\gamma} := \boldsymbol{\gamma}_h - \boldsymbol{\gamma}_I$, $\delta_w := w_h - w_I$, $\boldsymbol{\theta}_h := \nabla w_h + \boldsymbol{\gamma}_h$, $\boldsymbol{\theta}_I := \nabla w_I + \boldsymbol{\gamma}_I$ and $\boldsymbol{\delta_\theta} := \boldsymbol{\theta}_h - \boldsymbol{\theta}_I$. Thanks to Lemma 3.3 and equations (3.14), (3.9), (3.10) we have that

$$\begin{aligned}
\beta|||(w_h - w_I), (\boldsymbol{\gamma}_h - \boldsymbol{\gamma}_I)|||^2 &\leq a_h(\boldsymbol{\theta}_h - \boldsymbol{\theta}_I, \boldsymbol{\delta_\theta}) + b_h(\boldsymbol{\gamma}_h - \boldsymbol{\gamma}_I, \boldsymbol{\delta_\gamma}) \\
&= a_h(\nabla w_h + \boldsymbol{\gamma}_h, \boldsymbol{\delta_\theta}) + b_h(\boldsymbol{\gamma}_h, \boldsymbol{\delta_\gamma}) - (a_h(\boldsymbol{\theta}_I, \boldsymbol{\delta_\theta}) + b_h(\boldsymbol{\gamma}_I, \boldsymbol{\delta_\gamma})) \\
&= \langle g_h, \delta_w \rangle_h - \sum_{E\in\mathcal{T}_h} \left(a_h^E(\boldsymbol{\theta}_I - \boldsymbol{\theta}_\Pi, \boldsymbol{\delta_\theta}) + a^E(\boldsymbol{\theta}_\Pi - \boldsymbol{\theta}, \boldsymbol{\delta_\theta}) + a^E(\boldsymbol{\theta}, \boldsymbol{\delta_\theta})\right) \\
&\qquad - \sum_{E\in\mathcal{T}_h} \left(b_h^E(\boldsymbol{\gamma}_I - \boldsymbol{\gamma}_0, \boldsymbol{\delta_\gamma}) + b^E(\boldsymbol{\gamma}_0 - \boldsymbol{\gamma}, \boldsymbol{\delta_\gamma}) + b^E(\boldsymbol{\gamma}, \boldsymbol{\delta_\gamma})\right) \\
&\leq T_1 + T_2 + T_3,
\end{aligned}$$

where

$$T_1 := \left|\langle g_h, \delta_w\rangle_h - (g, \delta_w)_{0,\Omega}\right|, \qquad T_2 := \left|\sum_{E\in\mathcal{T}_h} \left(a_h^E(\boldsymbol{\theta}_I - \boldsymbol{\theta}_\Pi, \boldsymbol{\delta_\theta}) - a^E(\boldsymbol{\theta}_\Pi - \boldsymbol{\theta}, \boldsymbol{\delta_\theta})\right)\right|,$$

$$T_3 := = \left|\sum_{E\in\mathcal{T}_h} \left(b_h^E(\boldsymbol{\gamma}_I - \boldsymbol{\gamma}_0, \boldsymbol{\delta_\gamma}) - b^E(\boldsymbol{\gamma}_0 - \boldsymbol{\gamma}, \boldsymbol{\delta_\gamma})\right)\right|.$$

We now bound each term T_i, $i = 1, 2, 3$, with a constant C independent of h and t.

First, we bound the term T_2. Using (3.11), the fact that bilinear form $a(\cdot,\cdot)$ is bounded and finally adding and subtracting $\boldsymbol{\theta}$, we obtain

$$\begin{aligned}
T_2 &\leq \sum_{E\in\mathcal{T}_h} \left|a_h^E(\boldsymbol{\theta}_I - \boldsymbol{\theta}_\Pi, \boldsymbol{\delta_\theta})\right| + \sum_{E\in\mathcal{T}_h} \left|a^E(\boldsymbol{\theta}_\Pi - \boldsymbol{\theta}, \boldsymbol{\delta_\theta})\right| \\
&\leq \sum_{E\in\mathcal{T}_h} C(\|\boldsymbol{\theta}_I - \boldsymbol{\theta}_\Pi\|_{1,E} + \|\boldsymbol{\theta}_\Pi - \boldsymbol{\theta}\|_{1,E})\|\boldsymbol{\delta_\theta}\|_{1,E} \\
&\leq \sum_{E\in\mathcal{T}_h} C(\|\boldsymbol{\theta}_I - \boldsymbol{\theta}\|_{1,E} + \|\boldsymbol{\theta}_\Pi - \boldsymbol{\theta}\|_{1,E})\|\boldsymbol{\delta_\theta}\|_{1,E}.
\end{aligned}$$

For the term T_3, using (3.12), the definition of bilinear form $b(\cdot,\cdot)$, the Cauchy–Schwarz inequality, and finally adding and subtracting $\boldsymbol{\gamma}$, we obtain

$$T_3 \leq \sum_{E\in\mathcal{T}_h} C(\|\boldsymbol{\gamma}_I - \boldsymbol{\gamma}\|_{0,E} + \|\boldsymbol{\gamma}_0 - \boldsymbol{\gamma}\|_{0,E})t^{-2}\|\boldsymbol{\delta_\gamma}\|_{0,E}.$$

Now, we bound T_1. Using the definition (3.13), and adding and subtracting $\bar{g}_E$ we rewrite the term as follows

$$\begin{aligned}
T_1 &= \left|\sum_{E\in\mathcal{T}_h} \left(\bar{g}_E \sum_{i=1}^{N_E} \delta_w(\mathsf{v}_i)\omega_E^i\right) - \sum_{E\in\mathcal{T}_h} \int_E g\delta_w\right| \\
&= \left|\sum_{E\in\mathcal{T}_h} \left(\bar{g}_E \sum_{i=1}^{N_E} \delta_w(\mathsf{v}_i)\omega_E^i - \int_E \bar{g}_E\delta_w\right) + \sum_{E\in\mathcal{T}_h} \left(\int_E (\bar{g}_E - g)(\delta_w - p)\right)\right|,
\end{aligned}$$

for any $p \in \mathbb{P}_0(E)$, where we have used the definition of $\bar{g}_E$. Therefore,

$$T_1 \leq \left|\sum_{E\in\mathcal{T}_h} \left(\bar{g}_E \sum_{i=1}^{N_E} \delta_w(\mathsf{v}_i)\omega_E^i - \int_E \bar{g}_E\delta_w\right)\right| + \sum_{E\in\mathcal{T}_h} \|g - \bar{g}_E\|_{0,E}\|\delta_w - p\|_{0,E} := T_1^a + T_1^b.$$

First, T_1^b is easily bounded. In fact, taking p as in Proposition 4.1, we obtain that

$$T_1^b \leq Ch\|g\|_{0,\Omega}\|\delta_w\|_{1,\Omega}.$$

In what follows we will manipulate the terms T_1^a: adding and subtracting $p_0 \in \mathbb{P}_0(E)$, and since the integration rule in (3.13) is exact for constant functions, we have

$$\begin{aligned} T_1^a &\leq \left|\sum_{E\in\mathcal{T}_h}\int_E \bar{g}_E(\delta_w - p_0)\right| + \left|\sum_{E\in\mathcal{T}_h}\left(\bar{g}_E\left(\sum_{i=1}^{N_E}(\delta_w - p_0)(\mathsf{v}_i)\omega_E^i\right)\right)\right| \\ &\leq \|g\|_{0,\Omega}\left(\sum_{E\in\mathcal{T}_h}\|\delta_w - p_0\|_{0,E}^2\right)^{1/2} + \sum_{E\in\mathcal{T}_h}|E|\bar{g}_E\|\delta_w - p_0\|_{L^\infty(\partial E)} \\ &\leq \|g\|_{0,\Omega}\left(\sum_{E\in\mathcal{T}_h}\|\delta_w - p_0\|_{0,E}^2\right)^{1/2} + \|g\|_{0,\Omega}\left(\sum_{E\in\mathcal{T}_h}h_E^2\|\delta_w - p_0\|_{L^\infty(\partial E)}^2\right)^{1/2}. \end{aligned}$$

We now recall that $\delta_w - p_0$ is a (continuous) piecewise polynomial on ∂E, and that the length of the edges of E is bounded from below in the sense of assumption $\mathbf{A}_1$. Therefore, we can apply Lemma 3.1 in [16], standard polynomial approximation estimates and a trace inequality to derive

$$\|\delta_w - p_0\|_{L^\infty(\partial E)} \leq C|\delta_w|_{1/2,\partial E} + h_E^{-1/2}\|\delta_w - p_0\|_{0,\partial E} \leq C|\delta_w|_{1/2,\partial E} \leq C|\delta_w|_{1,E}.$$

Hence, we obtain,

$$T_1^a \leq Ch\|g\|_{0,\Omega}|\delta_w|_{1,\Omega}.$$

Thus, since $|\delta_w|_{1,\Omega} \leq |||\delta_w, \boldsymbol{\delta}_{\boldsymbol{\gamma}}|||$, we have that

$$T_1 \leq T_1^a + T_1^b \leq Ch\|g\|_{0,\Omega}|||\delta_w, \boldsymbol{\delta}_{\boldsymbol{\gamma}}|||. \tag{4.1}$$

Therefore, by combining (4.1) with the above bounds for T_2 and T_3, we get

$$\begin{aligned} |||(w_h - w_I), (\boldsymbol{\gamma}_h - \boldsymbol{\gamma}_I)||| \leq & C\big(t^{-1}(\|\boldsymbol{\gamma} - \boldsymbol{\gamma}_I\|_{0,\Omega} + \|\boldsymbol{\gamma}_0 - \boldsymbol{\gamma}\|_{0,\Omega}) \\ & + \|\boldsymbol{\theta} - \boldsymbol{\theta}_I\|_{1,\Omega} + \|\boldsymbol{\theta}_\Pi - \boldsymbol{\theta}\|_{1,h,\Omega} + h\|g\|_{0,\Omega}\big). \end{aligned}$$

Hence, the proof follows from the bound above, the triangular inequality, the definition of $|||\cdot|||$ (see (2.4)), the definition of $\boldsymbol{\theta}_I$ and the inequality $\|\boldsymbol{\theta} - \boldsymbol{\theta}_I\|_{1,\Omega} \leq \|\nabla w - \nabla w_I\|_{1,\Omega} + \|\boldsymbol{\gamma} - \boldsymbol{\gamma}_I\|_{1,\Omega}$. In fact,

$$\begin{aligned} |||w - w_h, \boldsymbol{\gamma} - \boldsymbol{\gamma}_h||| \leq & |||w - w_I, \boldsymbol{\gamma} - \boldsymbol{\gamma}_I||| + |||w_I - w_h, \boldsymbol{\gamma}_I - \boldsymbol{\gamma}_h||| \\ \leq & C(t^{-1}\|\boldsymbol{\gamma} - \boldsymbol{\gamma}_I\|_{0,\Omega} + t^{-1}\|\boldsymbol{\gamma}_0 - \boldsymbol{\gamma}\|_{0,\Omega} + \|\boldsymbol{\gamma} - \boldsymbol{\gamma}_I\|_{1,\Omega} \\ & + h\|g\|_{0,\Omega} + \|\boldsymbol{\theta} - \boldsymbol{\theta}_\Pi\|_{1,h,\Omega} + \|\nabla w - \nabla w_I\|_{1,\Omega}). \end{aligned}$$

The proof is complete. □

The next step is to find appropriate terms $(w_I, \boldsymbol{\gamma}_I)$, $(w_\Pi, \boldsymbol{\gamma}_\Pi)$ and $\boldsymbol{\gamma}_0$ that can be used in Lemma 4.3 to prove the claimed convergence. As a preliminary construction, we introduce, for every vertex v of the mesh laying on $\partial\Omega$, the following function. Let e_v be any one of the two edges on $\partial\Omega$ sharing v, fixed once and for all; the only rule being that, if one of the two edges is in Γ_c and the other is not, then the one in Γ_c must be chosen. Then, we denote by $\boldsymbol{\varphi}_\mathsf{v}$ the unique (vector valued) polynomial of degree 2 living on e_v such that

$$\int_{e_\mathsf{v}} \mathbf{p}\cdot\boldsymbol{\varphi}_\mathsf{v} = \mathbf{p}(\mathsf{v}) \qquad \forall \mathbf{p} \in [\mathbb{P}_2(e_\mathsf{v})]^2. \tag{4.2}$$

Then, for the term $w_I \in W_h$, we have the following result.

PROPOSITION 4.4. *There exists a positive constant C, such that for every $v \in H^3(\Omega)$ there exists $v_I \in W_h$ that satisfies*

$$|v - v_I|_{l,\Omega} \leq C h_E^{3-l} |v|_{3,\Omega}, \quad l = 0, 1, 2.$$

Proof. Given $v \in H^3(\Omega)$, we consider $v_\Pi \in L^2(\Omega)$ defined on each $E \in \mathcal{T}_h$ so that $v_\Pi|_E \in \mathbb{P}_2(E)$ and the estimate of Proposition 4.1 holds true.

For each polygon $E \in \mathcal{T}_h$, consider the triangulation $\mathcal{T}_h^E$ obtained by joining each vertex of E with the midpoint of the ball with respect to which E is starred. Let $\widehat{\mathcal{T}}_h := \bigcup_{E \in \mathcal{T}_h} \mathcal{T}_h^E$. Since we are assuming $\mathbf{A}_1$ and $\mathbf{A}_2$, $\left\{\widehat{\mathcal{T}}_h\right\}_h$ is a shape-regular family of triangulations of Ω.

Let v_c be the reduced Hsieh-Clough-Tocher triangle (see [25, 26]) interpolant of v over $\widehat{\mathcal{T}}_h$, slightly modified as follows. For the nodes on the boundary, the value of ∇v_c is given by

$$\nabla v_c(\mathsf{v}) := \int_{e_\mathsf{v}} \nabla v_c \cdot \boldsymbol{\varphi}_\mathsf{v},$$

see (4.2), while the values of the remaining degrees of freedom is the same as in the original version. This is a modification, in the spirit of the Scott-Zhang interpolation [39], of the standard nodal value; the motivation for such modification is not related directly to the present result (that would hold also with the original HCT interpolant) and will be clearer in the sequel. This modified version still satisfies similar approximation properties with respect the original version [25, 26]; we omit the standard proof and simply state the result:

$$|v - v_c|_{l,\Omega} \leq C h_E^{3-l} |v|_{3,\Omega} \quad l = 0, 1, 2. \tag{4.3}$$

Now, for each $E \in \mathcal{T}_h$, we define $v_I|_E \in H^2(E)$ as the solution of the following problem:

$$\begin{cases} -\Delta^2 v_I = -\Delta^2 v_\Pi & \text{in } E, \\ v_I = v_c & \text{on } \partial E, \\ \partial_{\boldsymbol{n}} v_I = \partial_{\boldsymbol{n}} v_c & \text{on } \partial E. \end{cases}$$

Note that $v_I|_E \in W_h^E$. Moreover, although v_I is defined locally, since on the boundary of each element it coincides with v_c which belongs to $H^2(\Omega)$, we have that also v_I belongs to $H^2(\Omega)$ and, hence, $v_I \in W_h$.

According to the above definition we have that

$$\begin{cases} -\Delta^2 (v_\Pi - v_I) = 0 & \text{in } E, \\ v_\Pi - v_I = v_\Pi - v_c & \text{on } \partial E, \\ \partial_{\boldsymbol{n}} (v_\Pi - v_I) = \partial_{\boldsymbol{n}} (v_\Pi - v_c) & \text{on } \partial E, \end{cases}$$

and, hence, it is easy to check that

$$\begin{aligned} |v_\Pi - v_I|_{2,E} &= \inf \left\{ |z|_{2,E}\,,\ z \in H^2(E) :\ z = v_\Pi - v_c \ \text{ on } \partial E \text{ and } \ \partial_{\boldsymbol{n}} z = \partial_{\boldsymbol{n}} (v_\Pi - v_c) \ \text{ on } \partial E \right\} \\ &\leq |v_\Pi - v_c|_{2,E}\,. \end{aligned}$$

Therefore,

$$\begin{aligned} |v - v_I|_{2,E} &\leq |v - v_\Pi|_{2,E} + |v_\Pi - v_I|_{2,E} \\ &\leq |v - v_\Pi|_{2,E} + |v_\Pi - v_c|_{2,E} \\ &\leq 2\,|v - v_\Pi|_{2,E} + |v - v_c|_{2,E}\,. \end{aligned}$$

By summing on all the elements and recalling (4.3) (plus standard approximation estimates for polynomials on polygons) we obtain

$$|v - v_I|_{2,\Omega} \leq C\big(|v - v_\Pi|_{2,\Omega} + |v - v_{\rm c}|_{2,\Omega} \big) \leq Ch|v|_{3,\Omega}.$$

Moreover, from the above bound and (recalling that $\partial_{\boldsymbol{n}}(v_I - v_{\rm c}) = 0$ and $(v_I - v_{\rm c}) = 0$ on ∂E) a Poincaré-type inequality, we have

$$\begin{aligned} |v - v_I|_{1,E} &\leq |v - v_{\rm c}|_{1,E} + |v_{\rm c} - v_I|_{1,E} \leq |v - v_{\rm c}|_{1,E} + Ch_E\, |v_{\rm c} - v_I|_{2,E} \\ &\leq |v - v_{\rm c}|_{1,E} + Ch_E\, |v - v_{\rm c}|_{2,E} + Ch_E\, |v - v_I|_{2,E}\,, \end{aligned}$$

so that, summing on all the elements and using the bounds above,

$$|v - v_I|_{1,\Omega} \leq Ch^2\, |v|_{3,\Omega}\,.$$

By an analogous argument one obtains

$$\|v - v_I\|_{0,\Omega} \leq C\big(\|v - v_{\rm c}\|_{0,\Omega} + h\, |v_{\rm c} - v_I|_{1,\Omega}\big) \leq Ch^3\, |v|_{3,\Omega}\,,$$

which allows us to complete the proof. □

Finally, we present the following result for the approximation properties of the space $\mathbf{V}_h$.

PROPOSITION 4.5. *There exists $C > 0$ such that for every $\boldsymbol{\tau} \in [H^s(\Omega)]^2$ with $s \in [1, 2]$ there exists $\boldsymbol{\tau}_I \in \mathbf{V}_h$ that satisfies*

$$\|\boldsymbol{\tau} - \boldsymbol{\tau}_I\|_{0,\Omega} + h|\boldsymbol{\tau} - \boldsymbol{\tau}_I|_{1,\Omega} \leq Ch^s|\boldsymbol{\tau}|_{s,\Omega}.$$

Proof. We refer the reader to Section 3.2 for the definition of the degrees of freedom of $\mathbf{V}_h$ and define $\boldsymbol{\tau}_I$ as follows. All degrees of freedom associated to internal vertices are calculated as an integral average of $\boldsymbol{\tau}$ on the elements sharing the vertex (as in standard Clément interpolation). All the vertex boundary values are taken as (see (4.2))

$$\boldsymbol{\tau}_I(\mathsf{v}) = \int_{e_\mathsf{v}} \boldsymbol{\tau} \cdot \boldsymbol{\varphi}_\mathsf{v}.$$

Finally, the edge degrees of freedom are computed directly by

$$\frac{1}{|e|}\int_e \boldsymbol{\tau}_I \cdot \boldsymbol{t} = \frac{1}{|e|}\int_e \boldsymbol{\tau} \cdot \boldsymbol{t} \quad \forall \text{ edge } e \in \mathcal{T}_h.$$

The rest of the proof is omitted since it follows repeating essentially the same argument used to establish [12, Proposition 4.1]. □

According to the above results, we are able to establish the convergence of the Virtual Element scheme presented in Problem 3.1.

THEOREM 4.6. *Let $(w, \boldsymbol{\gamma}) \in \boldsymbol{X}$ and $(w_h, \boldsymbol{\gamma}_h) \in \boldsymbol{X}_h$ be the unique solutions of the continuous and discrete problems, respectively. Assume that $(w, \boldsymbol{\gamma}) \in (H^3(\Omega), [H^2(\Omega)]^2)$. Then, there exists $C > 0$ independent of h, g and t such that*

$$|||w - w_h, \boldsymbol{\gamma} - \boldsymbol{\gamma}_h||| \leq Ch\left(t^{-1}|\boldsymbol{\gamma}|_{1,\Omega} + |\boldsymbol{\theta}|_{2,\Omega} + |w|_{3,\Omega} + \|g\|_{0,\Omega}\right),$$

where $\boldsymbol{\theta} := \nabla w + \boldsymbol{\gamma}$.

Proof. The proof follows from Lemma 4.3 and Propositions 4.1, 4.2, 4.4 and 4.5. In fact,

$$\begin{aligned} |||w - w_h, \boldsymbol{\gamma} - \boldsymbol{\gamma}_h||| \leq& C\Big(t^{-1}(\|\boldsymbol{\gamma} - \boldsymbol{\gamma}_I\|_{0,\Omega} + \|\boldsymbol{\gamma}_0 - \boldsymbol{\gamma}\|_{0,h,\Omega}) + \|\boldsymbol{\gamma} - \boldsymbol{\gamma}_I\|_{1,\Omega} \\ &+ h\|g\|_{0,\Omega} + \|\boldsymbol{\theta} - \boldsymbol{\theta}_\Pi\|_{1,h,\Omega} + \|\nabla w - \nabla w_I\|_{1,\Omega}\Big) \\ \leq& Ch\left(t^{-1}|\boldsymbol{\gamma}|_{1,\Omega} + |\boldsymbol{\theta}|_{2,\Omega} + |w|_{3,\Omega} + \|g\|_{0,\Omega}\right), \end{aligned}$$

where we have used that $\boldsymbol{\gamma} = \boldsymbol{\theta} - \nabla w$ so that $|\boldsymbol{\gamma}|_{2,\Omega} \leq |w|_{3,\Omega} + |\boldsymbol{\theta}|_{2,\Omega}$. Thus, we conclude the proof. ∎

Remark 4.1. *It is easy to check that the couple $(w_I, \boldsymbol{\gamma}_I)$ used in Theorem 4.6 (accordingly to the interpolants definition given in Propositions 4.4 and 4.5) does actually satisfy the boundary conditions and is thus in $\boldsymbol{X}_h$. Indeed, the condition $w_I = 0$ on $\Gamma_c \cup \Gamma_s$ follows immediately from the analogous one for w. The condition $\nabla w_I + \boldsymbol{\gamma}_I = \mathbf{0}$ on Γ_c can be easily derived from the analogous one for $(w, \boldsymbol{\gamma})$ combined with our choice for the boundary node interpolation and the definition of the discrete spaces.*

Remark 4.2. *We note that Theorem 4.6 provides also an error estimate for the rotations in $H^1(\Omega)$-norm.*

In what follows, we restrict our analysis considering clamped boundary conditions on the whole boundary, essentially to exploit the associated regularity properties of the continuous solution of the Reissner-Mindlin equations. Nevertheless, the analysis in what follows can be straightforwardly extended to other boundary conditions.

Now, we present the following result which establish an improve error estimate for rotations in $L^2(\Omega)$-norm and the deflection in $H^1(\Omega)$-norm.

PROPOSITION 4.7. *Assume that the hypotheses of Theorem 4.6 hold. Moreover, assume that the domain Ω be either regular, or piecewise regular and convex, that $g \in H^1(E)$ for all $E \in \mathcal{T}_h$ and that $\Gamma_c = \Gamma$. Then, for any $(w_\Pi, \boldsymbol{\gamma}_\Pi, \boldsymbol{\gamma}_0) \in [L^2(\Omega)]^5$ such that $w_\Pi|_E \in \mathbb{P}_2(E)$, $\boldsymbol{\gamma}_\Pi|_E \in [\mathbb{P}_1(E)]^2$ and $\boldsymbol{\gamma}_0|_E \in [\mathbb{P}_0(E)]^2$ for all $E \in \mathcal{T}_h$, there exists $C > 0$ independent of h, g and t such that*

$$\|\boldsymbol{\theta} - \boldsymbol{\theta}_h\|_{0,\Omega} \leq C(h+t)\left(|||w - w_h, \boldsymbol{\gamma} - \boldsymbol{\gamma}_h||| + h\|g\|_{1,h,\Omega} + \|\nabla w - \nabla w_\Pi\|_{1,h,\Omega} + \|\boldsymbol{\gamma} - \boldsymbol{\gamma}_\Pi\|_{1,h,\Omega} + t^{-1}\|\boldsymbol{\gamma} - \boldsymbol{\gamma}_0\|_{0,\Omega}\right); \tag{4.4}$$

$$\|w - w_h\|_{1,\Omega} \leq C(\|\boldsymbol{\theta} - \boldsymbol{\theta}_h\|_{0,\Omega} + \|\boldsymbol{\gamma} - \boldsymbol{\gamma}_h\|_{0,\Omega}). \tag{4.5}$$

Proof. The core of the proof is based on a duality argument. We first establish (4.4). We begin by introducing the following well-posed auxiliary problem: Find $(\widetilde{w}, \widetilde{\boldsymbol{\gamma}}) \in \boldsymbol{X}$ such that

$$a(\nabla\widetilde{w} + \widetilde{\boldsymbol{\gamma}}, \nabla v + \boldsymbol{\tau}) + b(\widetilde{\boldsymbol{\gamma}}, \boldsymbol{\tau}) = (\boldsymbol{\theta} - \boldsymbol{\theta}_h, \nabla v + \boldsymbol{\tau})_{0,\Omega} \quad \forall (v, \boldsymbol{\tau}) \in \boldsymbol{X}. \tag{4.6}$$

The following regularity result for the solution of problem above holds (see [34, Theorem 2.1]):

$$\|\widetilde{w}^1\|_{3,\Omega} + t^{-1}\|\widetilde{w}^2\|_{2,\Omega} + t^{-1}\|\widetilde{\boldsymbol{\gamma}}\|_{1,\Omega} \leq C\|\boldsymbol{\theta} - \boldsymbol{\theta}_h\|_{0,\Omega}, \tag{4.7}$$

where $\widetilde{w}^1$ is the solution of the Kirchhoff limit problem and $\widetilde{w}^2 := \widetilde{w} - \widetilde{w}^1$. Let $(\widetilde{w}_I^1, \widetilde{\boldsymbol{\gamma}}_I) \in \boldsymbol{X}_h$ be the interpolant of $(\widetilde{w}^1, \widetilde{\boldsymbol{\gamma}})$ given by Propositions 4.4 and 4.5, respectively. Therefore, the above regularity result yield immediately:

$$\|\widetilde{w}^1 - \widetilde{w}_I^1\|_{1,\Omega} + h\|\widetilde{w}^1 - \widetilde{w}_I^1\|_{2,\Omega} + t^{-1}h\|\widetilde{\boldsymbol{\gamma}} - \widetilde{\boldsymbol{\gamma}}_I\|_{0,\Omega} \leq h^2\|\boldsymbol{\theta} - \boldsymbol{\theta}_h\|_{0,\Omega}, \tag{4.8}$$

$$\|\widetilde{w}^2\|_{2,\Omega} + \|\widetilde{\boldsymbol{\gamma}} - \widetilde{\boldsymbol{\gamma}}_I\|_{1,\Omega} \leq t\|\boldsymbol{\theta} - \boldsymbol{\theta}_h\|_{0,\Omega}. \tag{4.9}$$

Next, choosing $v := (w - w_h)$ and $\boldsymbol{\tau} = (\boldsymbol{\gamma} - \boldsymbol{\gamma}_h)$ in (4.6), so that $\nabla v + \boldsymbol{\tau} = \boldsymbol{\theta} - \boldsymbol{\theta}_h$, and then adding and subtracting the term $\nabla\widetilde{w}_I^1 + \widetilde{\boldsymbol{\gamma}}_I$, we obtain

$$\begin{aligned}\|\boldsymbol{\theta} - \boldsymbol{\theta}_h\|_{0,\Omega}^2 &= a(\boldsymbol{\theta} - \boldsymbol{\theta}_h, \nabla\widetilde{w} + \widetilde{\boldsymbol{\gamma}} - \nabla\widetilde{w}_I^1 + \widetilde{\boldsymbol{\gamma}}_I) + a(\boldsymbol{\theta} - \boldsymbol{\theta}_h, \nabla\widetilde{w}_I^1 + \widetilde{\boldsymbol{\gamma}}_I) \\ &\quad + b(\boldsymbol{\gamma} - \boldsymbol{\gamma}_h, \widetilde{\boldsymbol{\gamma}} - \widetilde{\boldsymbol{\gamma}}_I) + b(\boldsymbol{\gamma} - \boldsymbol{\gamma}_h, \widetilde{\boldsymbol{\gamma}}_I) \\ &\leq |||w - w_h, \boldsymbol{\gamma} - \boldsymbol{\gamma}_h||| \, |||\widetilde{w} - \widetilde{w}_I^1, \widetilde{\boldsymbol{\gamma}} - \widetilde{\boldsymbol{\gamma}}_I||| + \left|a(\boldsymbol{\theta} - \boldsymbol{\theta}_h, \nabla\widetilde{w}_I^1 + \widetilde{\boldsymbol{\gamma}}_I) + b(\boldsymbol{\gamma} - \boldsymbol{\gamma}_h, \widetilde{\boldsymbol{\gamma}}_I)\right|,\end{aligned} \tag{4.10}$$

where we have used that the bilinear forms are bounded uniformly in t with respect to the $|||\cdot|||$ norm. Now, we bound each term on the right hand side above. For the first term we have, using (4.8) and (4.9),

$$\begin{aligned}|||\widetilde{w} - \widetilde{w}_I^1, \widetilde{\boldsymbol{\gamma}} - \widetilde{\boldsymbol{\gamma}}_I|||^2 &\leq C\left(\|\widetilde{w} - \widetilde{w}_I^1\|_{2,\Omega}^2 + t^{-2}\|\widetilde{\boldsymbol{\gamma}} - \widetilde{\boldsymbol{\gamma}}_I\|_{0,\Omega}^2 + \|\widetilde{\boldsymbol{\gamma}} - \widetilde{\boldsymbol{\gamma}}_I\|_{1,\Omega}^2\right) \\ &\leq C\left(\|\widetilde{w}^1 - \widetilde{w}_I^1\|_{2,\Omega}^2 + \|\widetilde{w}^2\|_{2,\Omega}^2 + t^{-2}\|\widetilde{\boldsymbol{\gamma}} - \widetilde{\boldsymbol{\gamma}}_I\|_{0,\Omega}^2 + \|\widetilde{\boldsymbol{\gamma}} - \widetilde{\boldsymbol{\gamma}}_I\|_{1,\Omega}^2\right) \\ &\leq C(h^2 + t^2)\|\boldsymbol{\theta} - \boldsymbol{\theta}_h\|_{0,\Omega}^2.\end{aligned}$$

Therefore

$$|||\widetilde{w}-\widetilde{w}_I^1,\widetilde{\boldsymbol{\gamma}}-\widetilde{\boldsymbol{\gamma}}_I|||\leq C(h+t)\|\boldsymbol{\theta}-\boldsymbol{\theta}_h\|_{0,\Omega}. \tag{4.11}$$

For the second term on the right hand of (4.10), since $(\widetilde{w}_I^1,\widetilde{\boldsymbol{\gamma}}_I)\in\boldsymbol{X}$, we have that (see Problems 2.2 and 3.1),

$$\begin{aligned}\left|a(\boldsymbol{\theta}-\boldsymbol{\theta}_h,\nabla\widetilde{w}_I^1+\widetilde{\boldsymbol{\gamma}}_I)+b(\boldsymbol{\gamma}-\boldsymbol{\gamma}_h,\widetilde{\boldsymbol{\gamma}}_I)\right|&=\left|(g,\widetilde{w}_I^1)_{0,\Omega}-a(\boldsymbol{\theta}_h,\nabla\widetilde{w}_I^1+\widetilde{\boldsymbol{\gamma}}_I)-b(\boldsymbol{\gamma}_h,\widetilde{\boldsymbol{\gamma}}_I)\right|\\&=\left|(g,\widetilde{w}_I^1)_{0,\Omega}-\left\langle g_h,\widetilde{w}_I^1\right\rangle_h+a_h(\boldsymbol{\theta}_h,\nabla\widetilde{w}_I^1+\widetilde{\boldsymbol{\gamma}}_I)+b_h(\boldsymbol{\gamma}_h,\widetilde{\boldsymbol{\gamma}}_I)-a(\boldsymbol{\theta}_h,\nabla\widetilde{w}_I^1+\widetilde{\boldsymbol{\gamma}}_I)-b(\boldsymbol{\gamma}_h,\widetilde{\boldsymbol{\gamma}}_I)\right|\\&\leq B_1+B_2,\end{aligned} \tag{4.12}$$

where

$$B_1:=\left|\left(g,\widetilde{w}_I^1\right)_{0,\Omega}-\left\langle g_h,\widetilde{w}_I^1\right\rangle_h\right|$$

and

$$B_2:=\left|a_h(\boldsymbol{\theta}_h,\nabla\widetilde{w}_I^1+\widetilde{\boldsymbol{\gamma}}_I)-a(\boldsymbol{\theta}_h,\nabla\widetilde{w}_I^1+\widetilde{\boldsymbol{\gamma}}_I)+b_h(\boldsymbol{\gamma}_h,\widetilde{\boldsymbol{\gamma}}_I)-b(\boldsymbol{\gamma}_h\widetilde{\boldsymbol{\gamma}}_I)\right|.$$

We now bound B_1 and B_2 uniformly in t.

We begin with the term B_1. First adding and subtracting $\widetilde{w}^1$ we have

$$\begin{aligned}B_1&\leq\left|(g,\widetilde{w}_I^1-\widetilde{w}^1)_{0,\Omega}\right|+\left|(g,\widetilde{w}^1)_{0,\Omega}-\left\langle g_h,\widetilde{w}^1\right\rangle_h\right|+\left|\left\langle g_h,\widetilde{w}_I^1-\widetilde{w}^1\right\rangle_h\right|\\&\leq h^2\|g\|_{0,\Omega}|\widetilde{w}^1|_{2,\Omega}+\left|(g,\widetilde{w}^1)_{0,\Omega}-\left\langle g_h,\widetilde{w}^1\right\rangle_h\right|,\end{aligned} \tag{4.13}$$

where we have used the Cauchy-Schwarz inequality and Proposition 4.4 to bound the first term; note moreover that the last term on the right hand side above vanish as a consequence of (3.13) and the definition of $\widetilde{w}_I^1$:

$$\left|\left\langle g_h,\widetilde{w}_I^1-\widetilde{w}^1\right\rangle_h\right|=\left|\sum_{E\in\mathcal{T}_h}\left(\bar{g}_E\sum_{i=1}^{N_E}(\widetilde{w}_I^1-\widetilde{w}^1)(\mathsf{v}_i)\omega_E^i\right)\right|=0.$$

Now, we bound the second term on the right hand side of (4.13) and we follow similar steps as in Lemma 4.3 to derive (4.1). In fact, using the definition (3.13), and adding and subtracting g_h we rewrite the term as follows

$$\begin{aligned}\left|(g,\widetilde{w}^1)_{0,\Omega}-\left\langle g_h,\widetilde{w}^1\right\rangle_h\right|&=\left|\sum_{E\in\mathcal{T}_h}\int_E g\widetilde{w}^1-\sum_{E\in\mathcal{T}_h}\left(\bar{g}_E\sum_{i=1}^{N_E}\widetilde{w}^1(\mathsf{v}_i)\omega_E^i\right)\right|\\&\leq\left|\int_E\bar{g}_E\widetilde{w}^1-\sum_{E\in\mathcal{T}_h}\left(\bar{g}_E\sum_{i=1}^{N_E}\widetilde{w}^1(\mathsf{v}_i)\omega_E^i\right)\right|+\sum_{E\in\mathcal{T}_h}\|g-\bar{g}_E\|_{0,E}\|\widetilde{w}^1-p\|_{0,E},\end{aligned}$$

for any $p\in\mathbb{P}_0(E)$. Now, taking p as in Proposition 4.1 and using that $g|_E\in H^1(E)$ and [17, Lemma 4.3.8]. we have that

$$\left|(g,\widetilde{w}^1)_{0,\Omega}-\left\langle g_h,\widetilde{w}^1\right\rangle_h\right|\leq Ch^2\|g\|_{1,h,\Omega}\|\widetilde{w}^1\|_{1,\Omega}+\left|\int_E\bar{g}_E\widetilde{w}^1-\sum_{E\in\mathcal{T}_h}\left(\bar{g}_E\sum_{i=1}^{N_E}\widetilde{w}^1(\mathsf{v}_i)\omega_E^i\right)\right|=B_1^1+B_1^2. \tag{4.14}$$

In what follows we will manipulate the terms B_1^2: adding and subtracting $p_1\in\mathbb{P}_1(E)$, and the fact that (3.13) is exact for linear functions, we have

$$\begin{aligned}B_1^2&\leq\left|\sum_{E\in\mathcal{T}_h}\int_E\bar{g}_E(\widetilde{w}^1-p_1)\right|+\left|\sum_{E\in\mathcal{T}_h}\left(\bar{g}_E\left(\sum_{i=1}^{N_E}(\widetilde{w}^1-p_1)(\mathsf{v}_i)\omega_E^i\right)\right)\right|\\&\leq\|g\|_{0,\Omega}\left(\sum_{E\in\mathcal{T}_h}\|\widetilde{w}^1-p_1\|_{0,E}^2\right)^{1/2}+\|g\|_{0,\Omega}\left(\sum_{E\in\mathcal{T}_h}h_E^2\|\widetilde{w}^1-p_1\|_{\infty,E}^2\right)^{1/2}.\end{aligned} \tag{4.15}$$

By polynomial approximation results on star-shaped polygons we now have

$$\begin{aligned} \|\widetilde{w}^1 - p_1\|_{0,E} &\leq Ch_E^2 |\widetilde{w}^1|_{2,E}, \\ \|\widetilde{w}^1 - p_1\|_{\infty,E} &\leq Ch_E |\widetilde{w}^1|_{2,E}, \end{aligned} \tag{4.16}$$

where the first bound follows from Proposition 4.1 and the second one can be derived, for instance, using the following brief guidelines. Let B be the ball with the same center appearing in $\mathbf{A}_2$, but radius h_E. It clearly holds $E \subset B$. One can then extend the function $\widetilde{w}^1$ to a function (still denoted by $\widetilde{w}^1$) in $H^2(B)$ with a uniform bound $\|\widetilde{w}^1\|_{2,B} \leq C\|\widetilde{w}^1\|_{2,E}$ (see for instance [40], where we use also that due to $\mathbf{A}_2$ all the elements E of the mesh family are uniformly Lipshitz continuous). Then, the result follows from the analogous known result on balls and some very simple calculations. Hence, from (4.15) and (4.16), we obtain

$$B_1^2 \leq Ch^2 \|g\|_{0,\Omega} |\widetilde{w}^1|_{2,\Omega}. \tag{4.17}$$

Finally, from (4.13), (4.14) and (4.17) we have the following bound for the term B_1:

$$B_1 \leq Ch^2 \|g\|_{1,h,\Omega} \|\widetilde{w}^1\|_{2,\Omega} \leq Ch^2 \|g\|_{1,h,\Omega} \|\boldsymbol{\theta} - \boldsymbol{\theta}_h\|_{0,\Omega} \leq C(h+t)h \|g\|_{1,h,\Omega} \|\boldsymbol{\theta} - \boldsymbol{\theta}_h\|_{0,\Omega}.$$

Now, we bound the term B_2 in (4.12). First, we consider $(w_\Pi, \boldsymbol{\gamma}_\Pi, \boldsymbol{\gamma}_0) \in [L^2(\Omega)]^5$ such that $w_\Pi|_E \in \mathbb{P}_2(E)$, $\boldsymbol{\gamma}_\Pi|_E \in [\mathbb{P}_1(E)]^2$ and $\boldsymbol{\gamma}_0|_E \in [\mathbb{P}_0(E)]^2$. Moreover, we consider $\widetilde{w}_\Pi^1 \in L^2(\Omega)$ with $\widetilde{w}_\Pi^1|_E \in \mathbb{P}_2(E)$ and define $\boldsymbol{\theta}_\Pi := \nabla w_\Pi + \boldsymbol{\gamma}_\Pi$. Thus, using the consistency property we rewrite the term as follows

$$\begin{aligned} B_2 = \Big| & \sum_{E \in \mathcal{T}_h} \left(a_h^E(\boldsymbol{\theta}_h, \nabla \widetilde{w}_I^1 + \widetilde{\boldsymbol{\gamma}}_I - (\nabla \widetilde{w}_\Pi^1 + \widetilde{\boldsymbol{\gamma}}_\Pi)) + a_h^E(\boldsymbol{\theta}_h, \nabla \widetilde{w}_\Pi^1 + \widetilde{\boldsymbol{\gamma}}_\Pi) \right) \\ & - \sum_{E \in \mathcal{T}_h} \left(a^E(\boldsymbol{\theta}_h, \nabla \widetilde{w}_I^1 + \widetilde{\boldsymbol{\gamma}}_I - (\nabla \widetilde{w}_\Pi^1 + \widetilde{\boldsymbol{\gamma}}_\Pi)) + a^E(\boldsymbol{\theta}_h, \nabla \widetilde{w}_\Pi^1 + \widetilde{\boldsymbol{\gamma}}_\Pi) \right) \\ & + \sum_{E \in \mathcal{T}_h} \left(b_h^E(\boldsymbol{\gamma}_h, \widetilde{\boldsymbol{\gamma}}_I - \widetilde{\boldsymbol{\gamma}}_0) + b_h^E(\boldsymbol{\gamma}_h, \widetilde{\boldsymbol{\gamma}}_0) - b^E(\boldsymbol{\gamma}_h, \widetilde{\boldsymbol{\gamma}}_I - \widetilde{\boldsymbol{\gamma}}_0) - b^E(\boldsymbol{\gamma}_h, \widetilde{\boldsymbol{\gamma}}_0) \right) \Big| \\ = \Big| & \sum_{E \in \mathcal{T}_h} \left(a_h^E(\boldsymbol{\theta}_h - \boldsymbol{\theta}_\Pi, \nabla \widetilde{w}_I^1 + \widetilde{\boldsymbol{\gamma}}_I - (\nabla \widetilde{w}_\Pi^1 + \widetilde{\boldsymbol{\gamma}}_\Pi)) - a^E(\boldsymbol{\theta}_h - \boldsymbol{\theta}_\Pi, \nabla \widetilde{w}_I^1 + \widetilde{\boldsymbol{\gamma}}_I - (\nabla \widetilde{w}_\Pi^1 + \widetilde{\boldsymbol{\gamma}}_\Pi)) \right) \\ & + \sum_{E \in \mathcal{T}_h} \left(b_h^E(\boldsymbol{\gamma}_h - \boldsymbol{\gamma}_0, \widetilde{\boldsymbol{\gamma}}_I - \widetilde{\boldsymbol{\gamma}}_0) - b^E(\boldsymbol{\gamma}_h - \boldsymbol{\gamma}_0, \widetilde{\boldsymbol{\gamma}}_I - \widetilde{\boldsymbol{\gamma}}_0) \right) \Big|. \end{aligned}$$

Therefore, we have

$$\begin{aligned} B_2 &\leq C \left(\|\boldsymbol{\theta}_h - \boldsymbol{\theta}_\Pi\|_{1,h,\Omega} + t^{-1} \|\boldsymbol{\gamma}_h - \boldsymbol{\gamma}_0\|_{0,\Omega} \right) \times \\ &\qquad \left(\sum_{E \in \mathcal{T}_h} \|\nabla \widetilde{w}_I^1 - \nabla \widetilde{w}_\Pi^1\|_{1,E}^2 + \|\widetilde{\boldsymbol{\gamma}}_I - \widetilde{\boldsymbol{\gamma}}_\Pi\|_{1,E}^2 + t^{-2} \|\widetilde{\boldsymbol{\gamma}}_I - \widetilde{\boldsymbol{\gamma}}_0\|_{0,E}^2 \right)^{1/2} \\ &\leq C \left(\|\boldsymbol{\theta}_h - \boldsymbol{\theta}_\Pi\|_{1,h,\Omega} + t^{-1} \|\boldsymbol{\gamma}_h - \boldsymbol{\gamma}_0\|_{0,\Omega} \right) \left(h|\widetilde{w}^1|_{3,\Omega} + ht^{-1} |\widetilde{\boldsymbol{\gamma}}|_{1,\Omega} + |\widetilde{\boldsymbol{\gamma}}|_{1,\Omega} \right), \end{aligned}$$

where we have added and subtracted $\nabla \widetilde{w}^1$ and $\widetilde{\boldsymbol{\gamma}}$ and then we have used Propositions 4.4, 4.1, 4.5 and 4.2, respectively. Finally, using (4.7) and the triangular inequality we have

$$B_2 \leq C(h+t) \|\boldsymbol{\theta} - \boldsymbol{\theta}_h\|_{0,\Omega} \left(|||w - w_h, \boldsymbol{\gamma} - \boldsymbol{\gamma}_h||| + \|\boldsymbol{\theta} - \boldsymbol{\theta}_\Pi\|_{1,h,\Omega} + t^{-1} \|\boldsymbol{\gamma} - \boldsymbol{\gamma}_0\|_{0,\Omega} \right).$$

Hence, (4.4) follows from (4.10), combining the estimate (4.11), with the above bounds for B_1 and B_2 and the definition of $\boldsymbol{\theta}$. In fact, we obtain that

$$\begin{aligned} \|\boldsymbol{\theta} - \boldsymbol{\theta}_h\|_{0,\Omega} \leq C(h+t) \big(|||w - w_h, \boldsymbol{\gamma} - \boldsymbol{\gamma}_h||| + h\|g\|_{1,h,\Omega} + \|\nabla w - \nabla w_\Pi\|_{1,h,\Omega} \\ + \|\boldsymbol{\gamma} - \boldsymbol{\gamma}_\Pi\|_{1,h,\Omega} + t^{-1} \|\boldsymbol{\gamma} - \boldsymbol{\gamma}_0\|_{0,\Omega} \big). \end{aligned}$$

Finally, bound (4.5) follows from the Poincaré inequality and the triangular inequality we have that

$$\|w-w_h\|_{1,\Omega} \leq C\|\nabla w - \nabla w_h\|_{0,\Omega} = C\|\boldsymbol{\theta}-\boldsymbol{\gamma}-(\boldsymbol{\theta}_h-\boldsymbol{\gamma}_h)\|_{0,\Omega} \leq C(\|\boldsymbol{\theta}-\boldsymbol{\theta}_h\|_{0,\Omega}+\|\boldsymbol{\gamma}-\boldsymbol{\gamma}_h\|_{0,\Omega}).$$

The proof is complete. ∎

Finally, we obtain the following result.

COROLLARY 4.8. *Assume that the hypotheses of Theorem 4.6 hold. Moreover, assume that the domain Ω be either regular, or piecewise regular and convex, that $g \in H^1(E)$ for all $E \in \mathcal{T}_h$ and that $\Gamma_c = \Gamma$. Then, there exists $C > 0$ independent of h, g and t such that*

$$\|\boldsymbol{\theta}-\boldsymbol{\theta}_h\|_{0,\Omega} + \|w-w_h\|_{1,\Omega} \leq C(h+t)h\left(t^{-1}|\boldsymbol{\gamma}|_{1,\Omega} + |\boldsymbol{\theta}|_{2,\Omega} + |w|_{3,\Omega} + \|g\|_{1,h,\Omega}\right).$$

Proof. The proof follows directly from Proposition 4.7, combining Theorem 4.6, Propositions 4.1, 4.2 and the fact that $\|\boldsymbol{\gamma}-\boldsymbol{\gamma}_h\|_{0,\Omega} \leq t|||w-w_h, \boldsymbol{\gamma}-\boldsymbol{\gamma}_h|||$. ∎

Remark 4.3. *We note that the shear strain variable in the present paper is given by $\boldsymbol{\gamma} = \nabla w - \boldsymbol{\theta}$ and it is related with the usual scaled shear strain used in other Reissner-Mindlin contributions in the literature as follows $Q = t^{-2}\boldsymbol{\gamma}$. Since $t^{-1}\boldsymbol{\gamma} = tQ$ is a quantity that is known to be uniformly bounded in the correct Sobolev norms (see, e.g [5, 20]). Therefore, the factors t^{-1} appearing in Theorem 4.6 and Corollary 4.8 are not a source of locking.*

Remark 4.4. *We note that in our convergence results, in order to obtain the full convergence rate in h (independently of the thickness t) we need $|w|_{3,\Omega}$ to be bounded uniformly in t. Even in the presence of regular data, this condition is not always assured due to the presence of layers at the boundaries of the plate. Such small limitation of the method is related to the adopted formulation and is, somehow, the drawback related to the advantage of having a method with C^1 deflections, that is therefore able to give (at the limit for vanishing thickness) a Kirchhoff conforming solution. We finally note that, in practice, this kind of difficulty can be effectively dealt with by an ad-hoc refinement of the mesh near the boundaries of the plate.*

5. Numerical results. We report in this section some numerical examples which have allowed us to assess the theoretical results proved above. We have implemented in a MATLAB code our method on arbitrary polygonal meshes, by following the ideas proposed in [8]. To complete the choice of the VEM, we have to fix the bilinear forms $S^E(\cdot,\cdot)$ and $S_0^E(\cdot,\cdot)$ satisfying (3.7) and (3.8), respectively. Proceeding as in [8], a natural choice for $S^E(\cdot,\cdot)$ is given by

$$S^E(\boldsymbol{\gamma}_h,\boldsymbol{\tau}_h) := \sum_{i=1}^{2N_E} \boldsymbol{\gamma}_h(\mathsf{v}_i)\boldsymbol{\tau}_h(\mathsf{v}_i) + \sum_{j=1}^{N_E}\left(\frac{1}{|e_j|}\int_{e_j}\boldsymbol{\gamma}_h\cdot\boldsymbol{t}\right)\left(\frac{1}{|e_j|}\int_{e_j}\boldsymbol{\tau}_h\cdot\boldsymbol{t}\right), \quad \boldsymbol{\gamma}_h,\boldsymbol{\tau}_h \in \mathbf{V}_h^E,$$

while a choice for $S_0^E(\cdot,\cdot)$ is given by

$$S_0^E(\boldsymbol{\gamma}_h,\boldsymbol{\tau}_h) := \frac{h_E^2}{t^2}\left(\sum_{i=1}^{2N_E} \boldsymbol{\gamma}_h(\mathsf{v}_i)\boldsymbol{\tau}_h(\mathsf{v}_i) + \sum_{j=1}^{N_E}\left(\frac{1}{|e_j|}\int_{e_j}\boldsymbol{\gamma}_h\cdot\boldsymbol{t}\right)\left(\frac{1}{|e_j|}\int_{e_j}\boldsymbol{\tau}_h\cdot\boldsymbol{t}\right)\right), \quad \boldsymbol{\gamma}_h,\boldsymbol{\tau}_h \in \mathbf{V}_h^E.$$

The choices above are standard in the Virtual Element literature, and correspond to a scaled identity matrix in the space of the degree of freedom values.

To test the convergence properties of the method, we introduce the following discrete L^2-like norm: for any sufficiently regular function $\mathbf{v}$,

$$\|\mathbf{v}\|_{0,\Omega}^2 := \sum_{E\in\mathcal{T}_h}\left(|E|\sum_{i=1}^{N_E}(\mathbf{v}(\mathsf{v}_i))^2\right),$$

with $|E|$ being the area of element E. We also define the relative errors in discrete L^2-like norms (based on the vertex values):

$$(e_w)^2 := \frac{\displaystyle\sum_{E\in\mathcal{T}_h}\left(|E|\sum_{i=1}^{N_E}\left(w(\mathsf{v}_i)-w_h(\mathsf{v}_i)\right)^2\right)}{\displaystyle\sum_{E\in\mathcal{T}_h}\left(|E|\sum_{i=1}^{N_E}\left(w(\mathsf{v}_i)\right)^2\right)},$$

and the obvious analogs for $e_{\nabla w}$ and $e_{\boldsymbol{\theta}}$. Finally, we introduce the relative error in the energy norm

$$(\boldsymbol{\mathcal{E}})^2 := \frac{\mathcal{A}_h((w-w_h,\boldsymbol{\gamma}-\boldsymbol{\gamma}_h),(w-w_h,\boldsymbol{\gamma}-\boldsymbol{\gamma}_h))}{\mathcal{A}_h((w,\boldsymbol{\gamma}),(w,\boldsymbol{\gamma}))},$$

where $\mathcal{A}_h(\cdot,\cdot)$ corresponds to the discrete bilinear form on the left hand side of Problem 3.1.

5.1. Test 1:. As a test problem we have taken an isotropic and homogeneous plate $\Omega := (0,1)^2$, clamped on the whole boundary, for which the analytical solution is explicitly known (see [24]).

Choosing the transversal load g as:

$$\begin{aligned} g(x,y) = \frac{E}{12(1-\nu^2)}\big[&12y(y-1)(5x^2-5x+1)(2y^2(y-1)^2+x(x-1)(5y^2-5y+1)\\ &+12x(x-1)(5y^2-5y+1)(2x^2(x-1)^2+y(y-1)(5x^2-5x+1)\big], \end{aligned}$$

the exact solution of the problem is given by:

$$\begin{aligned} w(x,y) = &\frac{1}{3}x^3(x-1)^3y^3(y-1)^3\\ &-\frac{2t^2}{5(1-\nu)}\left[y^3(y-1)^3x(x-1)(5x^2-5x+1)+x^3(x-1)^3y(y-1)(5y^2-5y+1)\right], \end{aligned}$$

$$\boldsymbol{\theta}(x,y) = \begin{bmatrix} y^3(y-1)^3x^2(x-1)^2(2x-1) \\ x^3(x-1)^3y^2(y-1)^2(2y-1) \end{bmatrix}.$$

The shear modulus λ is given by $\lambda := \dfrac{5E}{12(1+\nu)}$ (choosing 5/6 as shear correction factor), while the material constants have been chosen $E=1$ and $\nu=0$.

We have tested the method by using different values of the plate thickness: $t=0.1$, $t=0.01$ and $t=0.001$. Moreover, we have used different families of meshes (see Figure 5.1):

- $\mathcal{T}_h^1$: triangular meshes;
- $\mathcal{T}_h^2$: trapezoidal meshes which consist of partitions of the domain into $N\times N$ congruent trapezoids, all similar to the trapezoid with vertices $(0,0)$, $(\frac{1}{2},0)$, $(\frac{1}{2},\frac{2}{3})$ and $(0,\frac{1}{3})$;
- $\mathcal{T}_h^3$: triangular meshes, considering the middle point of each edge as a new degree of freedom but moved randomly; note that these meshes contain non-convex elements.

The refinement parameter h used to label each mesh is $h=\max_{E\in\mathcal{T}_h} h_E$.

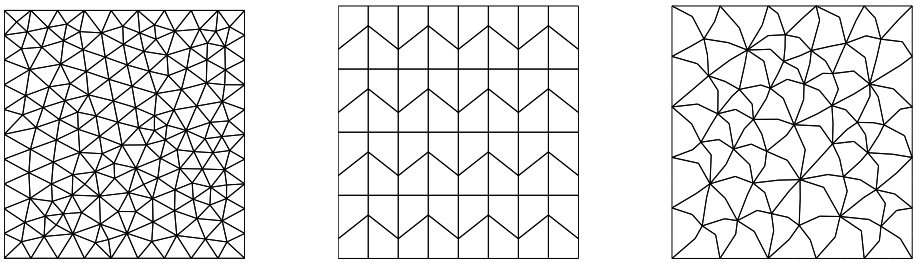

FIG. 5.1. *Sample meshes:* $\mathcal{T}_h^1$ *(left),* $\mathcal{T}_h^2$ *(middle) and* $\mathcal{T}_h^3$ *(right) with* $h = 0.1189$*,* $h = 0.1719$ *and* $h = 0.11078$*, respectively.*

We report in Table 5.1, Table 5.2 and Table 5.3 the relative errors in the discrete L^2-norm of w, ∇w and $\boldsymbol{\theta}$, together with the relative errors in the energy norm, for each family of meshes and different refinement levels. We consider different thickness: $t = 1.0e-01$, $t = 1.0e-02$ and $t = 1.0e-03$, respectively. We also include in these table the experimental rate of convergence.

TABLE 5.1
$\mathcal{T}_h^1$*: Computed error in* L^2*-norm with* $t = 1.0e-01$*,* $t = 1.0e-02$ *and* $t = 1.0e-03$*, respectively.*

error	$h = 0.1189$	$h = 0.05878$	$h = 0.03142$	$h = 0.01582$	$h = 0.008271$	Order
e_w	1.1084e-01	2.9410e-02	7.4232e-03	1.8414e-03	4.6791e-04	2.0627
$e_{\nabla w}$	1.3000e-01	4.1684e-02	1.3215e-02	4.2296e-03	1.5018e-03	1.6872
$e_{\boldsymbol{\theta}}$	8.8733e-02	2.2288e-02	5.4344e-03	1.3314e-03	3.3668e-04	2.1019
$\boldsymbol{\mathcal{E}}$	2.9935e-01	1.2776e-01	5.3946e-02	2.2765e-02	1.0702e-02	1.2625
e_w	1.0302e-01	2.6332e-02	6.4931e-03	1.5956e-03	4.0406e-04	2.0898
$e_{\nabla w}$	8.9532e-02	2.2548e-02	5.4769e-03	1.3430e-03	3.3972e-04	2.1023
$e_{\boldsymbol{\theta}}$	8.9247e-02	2.2442e-02	5.4452e-03	1.3345e-03	3.3748e-04	2.1036
$\boldsymbol{\mathcal{E}}$	1.7557e-01	8.5496e-02	4.1989e-02	2.0203e-02	1.0289e-02	1.0712
e_w	1.0296e-01	2.6311e-02	6.4884e-03	1.5960e-03	4.0430e-04	2.0893
$e_{\nabla w}$	8.9262e-02	2.2454e-02	5.4519e-03	1.3385e-03	3.3869e-04	2.1022
$e_{\boldsymbol{\theta}}$	8.9259e-02	2.2453e-02	5.4516e-03	1.3384e-03	3.3866e-04	2.1023
$\boldsymbol{\mathcal{E}}$	1.7332e-01	8.4751e-02	4.1677e-02	1.9984e-02	1.0143e-02	1.0719

TABLE 5.2
$\mathcal{T}_h^2$*: Computed error in* L^2*-norm with* $t = 1.0e-01$*,* $t = 1.0e-02$ *and* $t = 1.0e-03$*, respectively.*

error	$h = 0.1719$	$h = 0.0859$	$h = 0.0430$	$h = 0.0215$	$h = 0.0122$	Order
e_w	3.8903e-01	1.1104e-01	2.9582e-02	7.6148e-03	1.8676e-03	1.9103
$e_{\nabla w}$	4.1467e-01	1.3705e-01	4.3810e-02	1.4053e-02	4.6530e-03	1.6097
$e_{\boldsymbol{\theta}}$	3.6466e-01	9.7423e-02	2.4805e-02	6.2472e-03	1.5348e-03	1.9574
$\boldsymbol{\mathcal{E}}$	6.2673e-01	3.1044e-01	1.3447e-01	5.8121e-02	2.5266e-02	1.1580
e_w	3.7958e-01	1.0366e-01	2.6508e-02	6.6562e-03	1.6079e-03	1.9554
$e_{\nabla w}$	3.6633e-01	9.8309e-02	2.5015e-02	6.2782e-03	1.5342e-03	1.9594
$e_{\boldsymbol{\theta}}$	3.6589e-01	9.8016e-02	2.4903e-02	6.2447e-03	1.5252e-03	1.9611
$\boldsymbol{\mathcal{E}}$	4.1994e-01	1.6745e-01	7.4795e-02	3.6193e-02	1.8249e-02	1.1154
e_w	3.7950e-01	1.0361e-01	2.6499e-02	6.6620e-03	1.6120e-03	1.9545
$e_{\nabla w}$	3.6591e-01	9.8030e-02	2.4914e-02	6.2538e-03	1.5283e-03	1.9603
$e_{\boldsymbol{\theta}}$	3.6590e-01	9.8027e-02	2.4913e-02	6.2534e-03	1.5282e-03	1.9604
$\boldsymbol{\mathcal{E}}$	4.1544e-01	1.6465e-01	7.3602e-02	3.5478e-02	1.7716e-02	1.1213

TABLE 5.3
$\mathcal{T}_h^3$: Computed error in L^2-norm with $t = 1.0e-01$, $t = 1.0e-02$ and $t = 1.0e-03$, respectively.

error	$h = 0.1108$	$h = 0.05943$	$h = 0.02939$	$h = 0.01571$	$h = 0.007911$	Order
e_w	2.8478e-01	8.7688e-02	2.4214e-02	6.2665e-03	1.5694e-03	2.0614
$e_{\nabla w}$	3.1623e-01	1.2017e-01	4.0908e-02	1.3382e-02	4.4467e-03	1.6953
$e_{\boldsymbol{\theta}}$	2.5664e-01	7.4651e-02	1.9137e-02	4.7397e-03	1.1606e-03	2.1426
$\boldsymbol{\mathcal{E}}$	6.3713e-01	3.6532e-01	1.6896e-01	7.6472e-02	3.4702e-02	1.1691
e_w	2.6595e-01	7.4074e-02	1.9065e-02	4.7609e-03	1.1608e-03	2.1543
$e_{\nabla w}$	2.5677e-01	7.4955e-02	1.9117e-02	4.7777e-03	1.1667e-03	2.1435
$e_{\boldsymbol{\theta}}$	2.5625e-01	7.4605e-02	1.8981e-02	4.7359e-03	1.1552e-03	2.1466
$\boldsymbol{\mathcal{E}}$	3.7935e-01	1.9753e-01	9.5553e-02	4.8323e-02	2.3655e-02	1.1007
e_w	2.6642e-01	7.4576e-02	1.9021e-02	4.7417e-03	1.1613e-03	2.1801
$e_{\nabla w}$	2.5605e-01	7.4680e-02	1.9071e-02	4.7265e-03	1.1606e-03	2.1689
$e_{\boldsymbol{\theta}}$	2.5605e-01	7.4676e-02	1.9069e-02	4.7261e-03	1.1605e-03	2.1689
$\boldsymbol{\mathcal{E}}$	3.7438e-01	1.9044e-01	9.4471e-02	4.7568e-02	2.3429e-02	1.1081

It can be seen from Tables 5.1, 5.2 and 5.3 that the theoretical predictions of Section 4 are confirmed. In particular, we can appreciate a rate of convergence $O(h)$ for the energy norm $\boldsymbol{\mathcal{E}}$, that is equivalent to the $|||\cdot|||$ norm. This holds for all the considered meshes and thicknesses, thus also underlying the locking free nature of the scheme. Moreover, for sufficiently small t we also observe a clear rate of convergence $O(h^2)$ for for e_w, $e_{\nabla w}$ and $e_{\boldsymbol{\theta}}$, in accordance with Corollary 4.8.

5.2. Test 2:. As a second test, we investigate more in deep the locking-free character of the method, and also take the occasion for a comparison with the limit Kirchhoff model. It is well known (see [19]) that when t goes to zero the solution of the Reissner-Mindlin model converges to an identical Kirchhoff-Love solution: Find $w_0 \in H^2(\Omega)$ such that

$$\frac{E}{12(1-\nu^2)}\Delta^2 w_0 = g, \tag{5.1}$$

with the corresponding boundary conditions.

We have considered a rectangular plate $\Omega := (0,a)\times(0,b)$, simply supported on the whole boundary, and we have chosen the transversal load g as

$$g(x,y) = \sin\left(\frac{\pi}{a}x\right)\sin\left(\frac{\pi}{b}y\right).$$

Then, the analytical solution w_0 of problem (5.1) is given by

$$w_0(x,y) = \frac{12(1-\nu^2)}{E}\left(\pi^4\left(\frac{1}{a^2}+\frac{1}{b^2}\right)^2\right)^{-1}\sin\left(\frac{\pi}{a}x\right)\sin\left(\frac{\pi}{b}y\right).$$

The material constants have been chosen $E = 1$ and $\nu = 0.3$. Moreover, we have taken $a = 1$ and $b = 2$, and we have used three different families of meshes (see Figure 5.2):

- $\mathcal{T}_h^1$: triangular meshes;
- $\mathcal{T}_h^4$: hexagonal meshes;
- $\mathcal{T}_h^5$: Voronoi polygonal meshes.

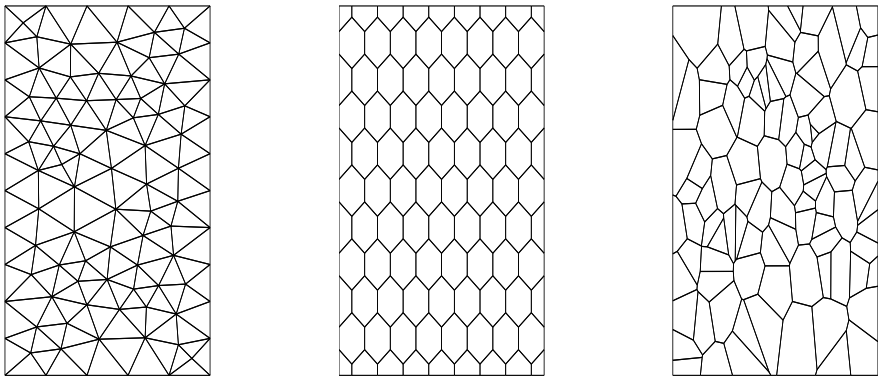

FIG. 5.2. *Sample meshes:* $\mathcal{T}_h^1$ *(left),* $\mathcal{T}_h^4$ *(middle) and* $\mathcal{T}_h^5$ *(right).*

Tables 5.4, 5.5 and 5.6 show an analysis for various thicknesses in order to assess the locking-free nature of the proposed method. We show the relative errors in the discrete L^2-norm of the deflection w for each family of meshes and different refinement levels and considering different thickness: $t = 1.0e-01$, $t = 1.0e-02$, $t = 1.0e-03$, $t = 1.0e-04$ and $t = 1.0e-05$, respectively.

It can be clearly seen from these tables that the proposed method is locking-free, since even for corse meshes the solution does not lock but approximates (for small t) the Kirchhoff solution.

TABLE 5.4
Computed error in e_w *by* $\mathcal{T}_h^1$.

$t\backslash h$	2.4495e-01	1.2706e-01	6.4686e-02	3.2407e-02	1.6166e-02
1.0e-01	8.6091e-03	4.0902e-02	6.0389e-02	7.1077e-02	7.5623e-02
1.0e-02	4.6875e-02	1.0335e-02	1.7984e-03	7.6646e-04	2.0123e-03
1.0e-03	4.7301e-02	1.0963e-02	2.7190e-03	6.6677e-04	1.3850e-04
1.0e-04	4.7305e-02	1.0969e-02	2.7284e-03	6.8234e-04	1.6637e-04
1.0e-05	4.7305e-02	1.0969e-02	2.7285e-03	6.8250e-04	1.6665e-04

TABLE 5.5
Computed error in e_w *by* $\mathcal{T}_h^4$.

$t\backslash h$	2.7813e-01	1.3086e-01	6.7301e-02	4.4428e-02	3.3163e-02
1.0e-01	8.3939e-02	5.9358e-02	6.2558e-02	6.7150e-02	6.9098e-02
1.0e-02	4.9794e-02	1.0178e-02	4.0223e-03	2.4758e-03	2.0948e-03
1.0e-03	4.9428e-02	9.5752e-03	3.1448e-03	1.3334e-03	7.3806e-04
1.0e-04	4.9424e-02	9.5691e-03	3.1358e-03	1.3211e-03	7.2280e-04
1.0e-05	4.9424e-02	9.5691e-03	3.1357e-03	1.3210e-03	7.2265e-04

TABLE 5.6
Computed error in e_w *by* $\mathcal{T}_h^5$.

$t\backslash h$	4.5918e-01	2.3481e-01	1.2942e-01	8.1744e-02	5.5071e-02
1.0e-01	2.7624e-02	4.0550e-02	4.6180e-02	6.5997e-02	6.9822e-02
1.0e-02	1.2695e-02	3.4544e-03	7.2182e-04	1.1407e-03	1.3932e-03
1.0e-03	1.2768e-02	3.0038e-03	3.8157e-04	6.4829e-05	4.5322e-05
1.0e-04	1.2768e-02	2.9994e-03	3.8727e-04	6.2480e-05	3.2567e-05
1.0e-05	1.2768e-02	2.9993e-03	3.8736e-04	6.2151e-05	3.1927e-05

REFERENCES

[1] B. Ahmad, A. Alsaedi, F. Brezzi, L. D. Marini and A. Russo, *Equivalent projectors for virtual element methods*, Comput. Math. Appl., **66**, (2013), pp. 376–391.

[2] P. F. Antonietti, L. Beirão da Veiga, D. Mora and M. Verani, *A stream virtual element formulation of the Stokes problem on polygonal meshes*, SIAM J. Numer. Anal., **52(1)**, (2014), pp. 386–404.

[3] P. F. Antonietti, L. Beirão da Veiga, S. Scacchi and M. Verani, *A C^1 virtual element method for the Cahn–Hilliard equation with polygonal meshes*, SIAM J. Numer. Anal., **54(1)**, (2016), pp. 36–56.

[4] P. F. Antonietti, P. Houston, M. Sarti and M. Verani, *Multigrid algorithms for hp-version interior penalty discontinuous Galerkin methods on polygonal and polyhedral meshes*, Pre-print arXiv:1412.0913 [math.NA] (2014).

[5] D.N. Arnold and R.S. Falk, *A uniformly accurate finite element method for the Reissner-Mindlin plate*, SIAM J. Numer. Anal., **26**, (1989), pp. 1276–1290.

[6] B. Ayuso de Dios, K. Lipnikov and G. Manzini, *The nonconforming virtual element method*, ESAIM Math. Model. Numer. Anal., **50(3)**, (2016), pp. 879–904.

[7] L. Beirão da Veiga, F. Brezzi, A. Cangiani, G. Manzini, L. D. Marini and A. Russo, *Basic principles of virtual element methods*, Math. Models Methods Appl. Sci., **23**, (2013), pp. 199–214.

[8] L. Beirão da Veiga, F. Brezzi, L. D. Marini and A. Russo, *The hitchhiker's guide to the virtual element method*, Math. Models Methods Appl. Sci., **24**, (2014), pp. 1541–1573.

[9] L. Beirão da Veiga, T.J.R. Hughes, J. Kiendl, C. Lovadina, J. Niiranen, A. Reali and H. Speleers, *A locking-free model for Reissner-Mindlin plates: analysis and isogeometric implementation via NURBS and triangular NURPS*, Math. Models Methods Appl. Sci., **25(8)**, (2015), pp. 1519–1551.

[10] L. Beirão da Veiga, K. Lipnikov and G. Manzini, *The Mimetic Finite Difference Method for Elliptic Problems*, Springer, MS&A, vol. **11**, 2014.

[11] L. Beirão da Veiga, C. Lovadina and D. Mora, *A virtual element method for elastic and inelastic problems on polytope meshes*, Comput. Methods Appl. Mech. Engrg., **295**, (2015) pp. 327–346.

[12] L. Beirão da Veiga, C. Lovadina and G. Vacca, *Divergence free Virtual Elements for the Stokes problem on polygonal meshes*, ESAIM Math. Model. Numer. Anal., DOI: http://dx.doi.org/10.1051/m2an/2016032 (2016).

[13] L. Beirão da Veiga, D. Mora, G. Rivera and R, Rodríguez, *A virtual element method for the acoustic vibration problem*, CI^{2}MA preprint 2015-44, available from http://www.ci2ma.udec.cl.

[14] M. F. Benedetto, S. Berrone, A. Borio, S. Pieraccini and S. Scialò, *A hybrid mortar virtual element method for discrete fracture network simulations*, J. Comput. Phys., **306**, (2016), pp. 148–166.

[15] M. F. Benedetto, S. Berrone, S. Pieraccini and S. Scialò, *The virtual element method for discrete fracture network simulations*, Comput. Methods Appl. Mech. Engrg., **280**, (2014), pp. 135–156.

[16] S. Bertoluzza, *Substructuring preconditioners for the three fields domain decomposition method*, Math. Comp. **73**, (2004), pp. 659–689.

[17] S. C. Brenner and R. L. Scott, *The Mathematical Theory of Finite Element Methods*, Springer, New York, 2008.

[18] F. Brezzi, R.S. Falk and L.D. Marini, *Basic principles of mixed virtual element methods*, ESAIM Math. Model. Numer. Anal., **48**, (2014), pp. 1227–1240.

[19] F. Brezzi and M. Fortin, *Mixed and Hybrid Finite Element Methods*, Springer-Verlag, New York (1991).

[20] F. Brezzi, M. Fortin and R. Stenberg, *Error analysis of mixed-interpolated elements for Reissner-Mindlin plates*, Math. Models Meth. Appl. Sci., **1**, (1991) pp. 125–151.

[21] F. Brezzi and L.D. Marini, *Virtual elements for plate bending problems*, Comput. Methods Appl. Mech. Engrg., **253**, (2012), pp. 455–462.

[22] E. Caceres and G.N. Gatica, *A mixed virtual element method for the pseudostress-velocity formulation of the Stokes problem*, IMA J. Numer. Anal., DOI:10.1093/imanum/drw002 (2016).

[23] A. Cangiani, E. H. Georgoulis and P. Houston, *hp-version discontinuous Galerkin methods on polygonal and polyhedral meshes*, Math. Models Methods Appl. Sci., **24(10)**, (2014), pp. 2009–2041.

[24] C. Chinosi and C. Lovadina, *Numerical analysis of some mixed finite element methods for Reissner-Mindlin plates*, Comput. Mech., **16(1)**, (1995), pp. 36–44.

[25] P. G. Ciarlet, *The Finite Element Method for Elliptic Problems*, SIAM, 2002.

[26] P. G. Ciarlet, *Interpolation error estimates for the reduced Hsieh–Clough–Tocher triangle*, Math. Comp., **32(142)**, (1978), pp. 335–344.

[27] D. Di Pietro and A. Ern, *A hybrid high-order locking-free method for linear elasticity on general meshes*, Comput. Methods Appl. Mech. Eng., **283**, (2015), pp. 1–21.

[28] R. Echter, B. Oesterle and M. Bischoff, *A hierarchic family of isogeometric shell finite elements*, Comput. Methods Appl. Mech. Engrg., **254**, (2013) pp. 170–180.

[29] R. Falk, *Finite elements for the Reissner-Mindlin plate*, D. Boffi and L. Gastaldi, editors, Mixed finite elements, compatibility conditions, and applications, Springer, Berlin, 2008, pp. 195–232.

[30] A. L. Gain, C. Talischi and G.H. Paulino, *On the virtual element method for three-dimensional linear elasticity problems on arbitrary polyhedral meshes*, Comput. Methods Appl. Mech. Engrg., **282**, (2014), pp. 132–160.

[31] V. Girault and P.A. Raviart, *Finite Element Methods for Navier-Stokes Equations*, Springer-Verlag, Berlin, 1986.

[32] Q. Long, P. B. Bornemann and F. Cirak, *Shear-flexible subdivision shells*, Internat. J. Numer. Methods Engrg., **90(13)**, (2012) pp. 1549–1577.

[33] C. Lovadina, *A brief overview of plate finite element methods*, Integral methods in science and engineering. Vol. 2, 261–280, Birkhäuser Boston, Inc., Boston, MA, 2010.
[34] M. Lyly, J. Niiranen and R. Stenberg, *A refined error analysis of MITC plate elements*, Math. Models Methods Appl. Sci., **16**, (2006), pp 967–977.
[35] D. Mora, G. Rivera and R. Rodríguez, *A virtual element method for the Steklov eigenvalue problem*, Math. Models Methods Appl. Sci., **25(8)**, (2015), pp. 1421–1445.
[36] G. H. Paulino and A. L. Gain, *Bridging art and engineering using Escher-based virtual elements*, Struct. Multidiscip. Optim., **51(4)**, (2015), pp. 867–883.
[37] I. Perugia, P. Pietra and A. Russo, *A plane wave virtual element method for the Helmholtz problem*, ESAIM Math. Model. Numer. Anal., **50(3)**, (2016), pp. 783–808.
[38] S. Rjasanow and S. Weisser, *Higher order BEM-based FEM on polygonal meshes*, SIAM J. Numer. Anal., **50(5)**, (2012), pp. 2357–2378.
[39] L. R. Scott and S. Zhang, *Finite element interpolation of nonsmooth functions satisfying boundary conditions*, Math. Comp. **54**, (1990), pp. 483–493.
[40] E. M. Stein, *Singular integrals and differentiability properties of functions*, volume 2. Princeton University Press, 1970.
[41] N. Sukumar and A. Tabarraei, *Conforming polygonal finite elements*, Internat. J. Numer. Methods Engrg., **61**, (2004), pp. 2045–2066.
[42] C. Talischi, G. H. Paulino, A. Pereira and I. F. M. Menezes, *Polygonal finite elements for topology optimization: A unifying paradigm*, Internat. J. Numer. Methods Engrg., **82(6)**, (2010), pp. 671–698.
[43] P. Wriggers, W. T. Rust and B. D. Reddy, *A virtual element method for contact*, Submitted for publication.

Centro de Investigación en Ingeniería Matemática (CI^{2}MA)

PRE-PUBLICACIONES 2016

2016-03 Gabriel N. Gatica: *A note on stable Helmholtz decompositions in 3D*

2016-04 Julio Aracena, Adrien Richard, Lilian Salinas: *Number of fixed points and disjoint cycles in monotone Boolean networks*

2016-05 Sophie Balemans, Raimund Bürger, Stefan Diehl, Pierre Francois, Julien Laurent, Florent Locatelli, Ingmar Nopens, Elena Torfs: *On constitutive functions for hindered settling velocity in 1-D settler models: selection of appropriate model structure*

2016-06 Anahi Gajardo, Vincent Nesme, Guillaume Theyssier: *Pre-expansivity in cellular automata*

2016-07 Eligio Colmenares, Michael Neilan: *Dual-mixed finite element methods for the stationary Boussinesq problem*

2016-08 Veronica Anaya, David Mora, Carlos Reales, Ricardo Ruiz-Baier: *Finite element methods for a stream-function – vorticity formulation of the axisymmetric Brinkman equations*

2016-09 Rommel Bustinza, Bibiana López-Rodríguez, Mauricio Osorio: *An a priori error analysis of an HDG method for an eddy current problem*

2016-10 Luis M. Castro, Víctor H. Lachos, Tsung-I Lin, Larissa A. Matos: *Heavy-tailed longitudinal regression models for censored data: A likelihood based perspective*

2016-11 Gabriel N. Gatica, Ricardo Ruiz-Baier, Giordano Tierra: *A posteriori error analysis of an augmented mixed method for the Navier-Stokes equations with nonlinear viscosity*

2016-12 Manuel Solano, Felipe Vargas: *A high order HDG method for Stokes flow in curved domains*

2016-13 Huangxin Chen, Weifeng Qiu, Ke Shi, Manuel Solano: *A superconvergent HDG method for the Maxwell equations*

2016-14 Lourenco Beirao-Da-Veiga, David Mora, Gonzalo Rivera: *A virtual element method for Reissner-Mindlin plates*

Para obtener copias de las Pre-Publicaciones, escribir o llamar a: Director, Centro de Investigación en Ingeniería Matemática, Universidad de Concepción, Casilla 160-C, Concepción, Chile, Tel.: 41-2661324, o bien, visitar la página web del centro: `http://www.ci2ma.udec.cl`







Centro de Investigación en
Ingeniería Matemática (CI²MA)
Universidad de Concepción

Casilla 160-C, Concepción, Chile
Tel.: 56-41-2661324/2661554/2661316
http://www.ci2ma.udec.cl